Thesis for the degree of Licentiate of Engineering

Solder Matrix Fiber Composite Thermal Interface Materials

Josef Hansson

Department of Microtechnology and Nanoscience - MC2
CHALMERS UNIVERSITY OF TECHNOLOGY
Göteborg, Sweden 2018

Solder Matrix Fiber Composite Thermal Interface Materials
JOSEF HANSSON

Chalmers University of Technology
Department of Microtechnology and Nanoscience - MC2
Electronic Materials and Systems Laboratory
SE–412 96 Göteborg, Sweden
Telephone + 46 (0) 31 – 772 1000

Licentiatavhandlingar vid Chalmers tekniska högskola
ISSN 1652-0769
Technical report MC2-397

Abstract

Overheating has been a problem for microelectronics devices for decades, and the problem is exacerbated by the continued trend of miniaturization of features and the corresponding increase in power density. Thermal interface materials (TIMs) target one of the main bottlenecks in heat transfer: the interface between two materials, such as between a heat-generating microchip and a heatsink. By filling out microgaps caused by the roughness of the mating surfaces, TIMs improve the heat transfer over the interface by orders of magnitude. Nonetheless, even with a TIM the interface can be a limiting factor for the overall cooling. Thus, the development of new and improved TIMs is a big challenge for the electronics field.

This thesis thoroughly reviews the overall status of the field of TIM research, and identifies three main tracks for novel research. First, particle laden polymers, which utilizes thermally conductive particles inside a polymer matrix which can conform to surfaces. Second, continuous metal phase TIM, which forms metallurgical bonds to both surfaces, and utilizes the inherently high thermal conductivity of metals. Third, carbon nanotube (CNT) array TIMs, which utilize the incredible thermal conductivity of CNTs. Here, an array of vertically aligned CNTs is used as nanosprings to connect the two surfaces together. In addition to these main tracks, various novel ideas based on polymers, metal and carbonaceous materials are explored.

From the reviewed categories, continuous metal phase TIM in the form of solder is already widely used in industry, but comes with severe drawbacks in terms of mechanical properties and handling issues. Solder matrix fiber composites (SMFCs) have been shown to address these challenges, but have so far required complicated procedures and components. In this thesis, we present the fabrication of a new SMFCs based on commercially available polymer and carbon fiber networks infiltrated with Sn-Ag-Cu alloy (SAC) or Indium using equipment for large volume production. The composite material exhibits similar thermal properties compared to pure solder, and mechanical properties that can be tailored towards specific applications. We also show that the handling properties of the SMFC allows it to be used in process flows where multiple reflow cycles are required, and can achieve a well-defined bond line thickness and good bonding using fluxless reflow under pressure.

Keywords: thermal management, thermal interface material, solder, composite materials.

List of Publications

Appended Papers

This thesis is based on the following papers:

Paper A. Novel nanostructured thermal interface materials: a review
Josef Hansson, Torbjörn Nilsson, Lilei Ye, Johan Liu
International Materials Reviews, 2017.

Paper B. Fabrication and Characterization of a Carbon Fiber Solder Composite Thermal Interface Material
Josef Hansson, Lilei Ye, Johan Liu
IMAPS Nordic Conference on Microelectronics Packaging (NordPac), Gothenburg, Sweden, 2017.

Paper C. Effect of fiber concentration on mechanical and thermal properties of a solder matrix fiber composite thermal interface material
Josef Hansson, Torbjörn Nilsson, Lilei Ye, Johan Liu
Submitted to Transactions on Components, Packaging and Manufacturing Technology, 2018.

Other Contributions

Double-Densified Vertically Aligned Carbon Nanotube Bundles for Application and Integration in 3D High Aspect Ratio TSV Interconnects
Wei Mu, Josef Hansson, Shuangxi Sun, Michael Edwards, Yifeng Fu, Kjell Jeppson, Johan Liu
IEEE 66th Electronic Components and Technology Conference, Las Vegas, NV, 2016.

A Review of Recent Progress of Thermal Interface Materials: From Research to Industrial Applications
Josef Hansson, Lilei Ye, Henric Rhedin, Johan Liu
2016 IMAPS Nordic Conference on Microelectronics Packaging, Tonsberg, Norway, 2016.

Review of current progress of thermal interface materials for electronics thermal management applications
Josef Hansson, Carl Zandén, Lilei Ye, Johan Liu
IEEE 16th International Conference on Nanotechnology (IEEE-NANO), Sendai, Japan, 2016.

Finite element analysis of bond line thickness and fiber distribution in solder based thermal interface materials
Maulik Satwara, Josef Hansson, Lilei Ye, Henric Rhedin, Johan Liu
2017 IMAPS Nordic Conference on Microelectronics Packaging (NordPac), Gothenburg, Sweden, 2017.

Synthesis of a Graphene Carbon Nanotube Hybrid Film by Joule Self-heating CVD for Thermal Applications
Josef Hansson, Majid Kabiri Samani, Andreas Nylander, Lilei Ye, Nan Wang, Torbjörn Nilsson, Johan Liu
IEEE 68th Electronic Components and Technology Conference, 2018.

List of Acronyms

TIM – Thermal Interface Material
PCB – Printed Circuit Board
CTE – Coefficient of Thermal Expansion
BGA – Ball Grid Array
IHS – Internal Heat Spreader
PCM – Phase Change Material
SEM – Scanning Electron Microscope
NW – Nanowire
SAC – Sn-Ag-Cu (Tin Silver Copper)
LMA – Low Melting point Alloy
CVD – Chemical Vapor Deposition
SMFNC – Solder Matrix Fiber Network Composite
CF – Carbon Fiber
PI – Polyimide
GO – Graphene Oxide

Contents

Chapter 1

Introduction

1.1 Background

The first and second law of thermodynamics state that energy is always conserved within a closed system, and that the entropy of a closed system always increases, respectively. In other words, that energy is never created or destroyed, only converted, and this conversion leads to a less ordered state. In general, the highest entropy state is the random movement of individual atoms, or in other words, heat. And as such, chemical and physical reactions tend to increase the temperature of the system.

Electrical currents are no exceptions, and, disregarding the case of superconductors, all electrical circuits create some amount of heat. In some cases, this is by design, but usually it is unwanted waste heat, which in certain applications can cause significant problems, in addition to the energy inefficiency. The field of microelectronics is one such field, the decreasing feature size and increasing density has increased the thermal waste generation to the point where active cooling solutions are necessary to prevent overheating of the active components. In fact, active cooling is responsible for a significant fraction of the total power consumption in modern data centers [1]. Even despite the active cooling solutions, thermal management presents a bottleneck towards further miniaturization. Therefore, there is a need for better materials to efficiently remove heat from heat generating components.

When designing the cooling solution for microelectronic systems, invariably, different materials and components will be included. Heat spreaders, heat pipes and heat sinks among others, can all have a place within the total system, and new materials and designs for all these components are continuously explored. However, regardless of the efficiency of individual components, in order to bring them together into a complete system, connections between different components and the heat source itself is required. Since the surfaces of components are never perfectly flat, a simple mechanical connection between two surfaces usually results in a very limited fraction of the total area of the surfaces in actual contact, with air trapped between the contacting peaks. This severely restricts the heat flow between them, to the point where these interfaces are significant bottlenecks for the heat conduction. In order to fill these air gaps, thermal interface materials (TIMs) are used. A TIM is a material, placed between connecting surfaces, that can conform to irregularities and fill out the air gaps in order to facilitate heat transfer.

A perfect TIM would fill out only the original air gaps with a material of a thermal conductivity as high as the mating materials. Naturally, such a material does not actually exist for most applications, and so the results will be a compromise between thermal conductivity, conformability, ease of application, cost, reliability, etc. In the end, despite the application of TIM, thermal interfaces can still represent a large part of the thermal budget for a system, and the development of better TIM is crucial for the continued overall development in the field of microelectronics[2].

This need has led to a large variety of solutions in use in industry for different applications, and an even larger variety being actively researched. As a researcher or someone working in the field, having a broad knowledge of different types of existing and future TIM is vital, including their properties, features and applications. As a part of this thesis, a systematic review over TIM research has been done, focusing especially on nanostructured materials.

One type of TIM of particular note for the scope of this thesis is the solder TIM. Here, a low melting point metal alloy is used to join two surfaces, in a similar manner to the attachment of electronic components on a printed circuit board (PCB). The molten metal can fill out surface irregularities, and when cooled and solidified, form metallurgical bonds to the joined surfaces. In addition, while the thermal conductivity of solder alloys are lower than most pure metals, it is still relatively high compared with most other TIM types.

However, solder can have reliability issues, due to its relatively high stiffness, which makes it unable to absorb the stress created when the two joining surfaces are of materials with different coefficient of thermal expansion (CTE), which can lead to delamination or crack formation. In addition, solder can be difficult to process on large areas, such as molten solder pumping out of the interface, or a slight imbalance can cause the thickness of the TIM layer, or the bond line thickness (BLT), to become uneven over the surface. This thesis concerns the effort to create a composite structure which retains the thermal and connecting properties of solder TIMs, while addressing the problems with using pure solder.

1.2 Outline

This thesis is divided into two parts. Chapter 2 introduces in detail the research area of thermal interface materials. First, the working principle of TIMs is introduced together with important properties and figures of merit which are relevant for TIM selection. Second, a brief overview of existing TIMs used in industry is provided. Finally, novel research on TIMs is presented, divided into four general areas, together with a review of the status of the respective areas in terms of progress and academic height.

The second part of this thesis, chapter 3, presents the experimental research into a specific type of TIM, the solder matrix fiber network composite (SMFC), which consists of a nonwoven horizontal randomly aligned fiber network inside a solder matrix. Two different kinds of fibers, silver coated nylon (PA6,6) and carbon fiber

(CF), and two different matrix alloys, Indium and Sn-Ag-Cu, are explored. The chapter details the fabrication of the composite materials, as well as the thermal and mechanical characterization of the TIM.

Chapter 2

Thermal Interface Materials

A surface is never completely flat, and will, at the microscopic scale, always have some degree of roughness. Pressing two such surfaces together will thus lead to a very limited contact, as seen in figure 2.1a. These contacting choke points will constrict the heat flux (red lines) and lead to a large temperature drop over the interface.

To reduce the temperature drop, a thermal interface material (TIM) can be placed in between mating surfaces to fill the trapped voids and increase the effective contact area. The thermal conductivity of the TIM is normally lower than the mating substrates, and for this reason an ideal TIM would only fill out the voids between the mating surfaces as seen in figure 2.1b. In reality, the application of a TIM will cause a gap between the surfaces, as seen in figure 2.1c, called the bond line thickness (BLT).

The most important figure of merit for a TIM is the thermal interface resistance (R_{TIM}), which is a measure on how difficult it is for heat to dissipate over the interface. It is related to the temperature drop (ΔT) over the interface according to Fourier's law as $\Delta T = R_{TIM}Q$, where Q is the heat flux. Minimizing R_{TIM} is

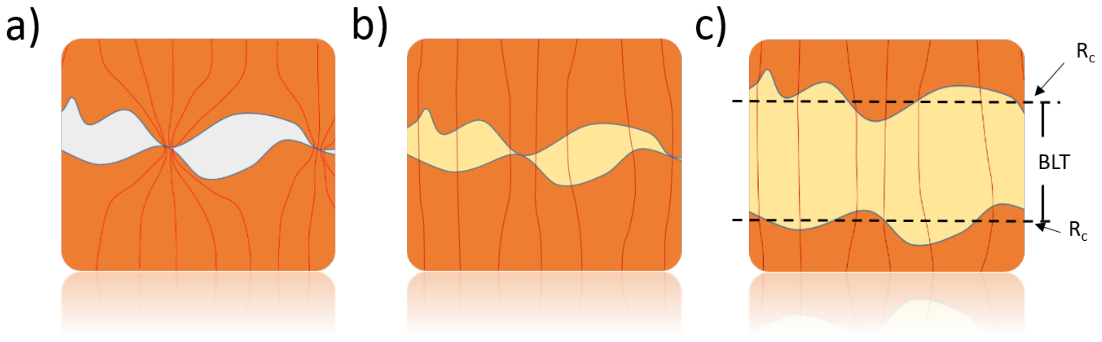

Figure 2.1: a) The principle for the heat flow in a bare interface. b) In ideal TIM filling out the remaining voids. c) A realistic TIM with a bond line thickness.

a general goal of thermal interface materials development. The thermal interface resistance can be divided into resistive components, for a TIM typically

$$R_{TIM} = R_{c_1} + \frac{BLT}{\lambda_{TIM}} + R_{c_2} \tag{2.1}$$

where R_{TIM} is the total thermal interface resistance, R_{c_1} and R_{c_2} is the contact resistances at the interface between the TIM and the two substrates, λ_{TIM} the thermal conductivity of the TIM and BLT is the bond line thickness i.e. the thickness of the TIM. Depending on the type of TIM and application, the different terms of the equation will have more or less impact on the overall performance, and when choosing or designing a TIM it is important to identify which parameters to address.

R_c - Between substrate and TIM there is a contact resistance depending on the thermal contact. This contact resistance depends on how well the TIM conforms to the substrate and fills out voids. It is affected by the compliancy of the TIM as well as how well it wets to the substrates, and is often related to the applied pressure. There is also a thermal boundary resistance between two different material even if atomically smooth, due to phonon or electron scattering at the interface. This effect is called Kapitza resistance[3].

BLT - The bond line thickness of the TIM is a measure of how separated the two surfaces are i.e. how thick the TIM is. As the TIM typically still has significantly lower thermal conductivity than either of the surfaces it is desirable to minimize the bond line thickness. In addition, lower BLT means less material used, and thus usually a lower cost as well. Ideally the TIM only fills out the voids in the original interface. However, in practice a very thin bond line can result in voiding due to uneven TIM coverage as well as reliability issues during thermal cycling due to mismatch in coefficient of thermal expansion (CTE).

For TIMs in liquid form, the BLT is influenced by the amount of material but also the viscosity of the material as well as clamping pressure. In addition, for TIM loaded with solid filler particles, the size of the fillers can introduce a limit on how thin BLT is possible. For a TIM applied as a pad the bond line thickness is limited by handling and mechanical requirements.

λ - The thermal conductivity of the thermal interface material is the measure on how well the material conducts heat within itself. The importance of a high thermal conductivity is proportional to the BLT i.e. for very low bond line thicknesses the contact resistance dominates over the resistance due to thermal conductivity, but for thick TIMs the thermal conductivity becomes a critical parameter.

Aside from the thermal performance, there are a number of considerations to take into account when choosing or developing TIMs. Examples include:

- If the TIM is electrically conductive or not.

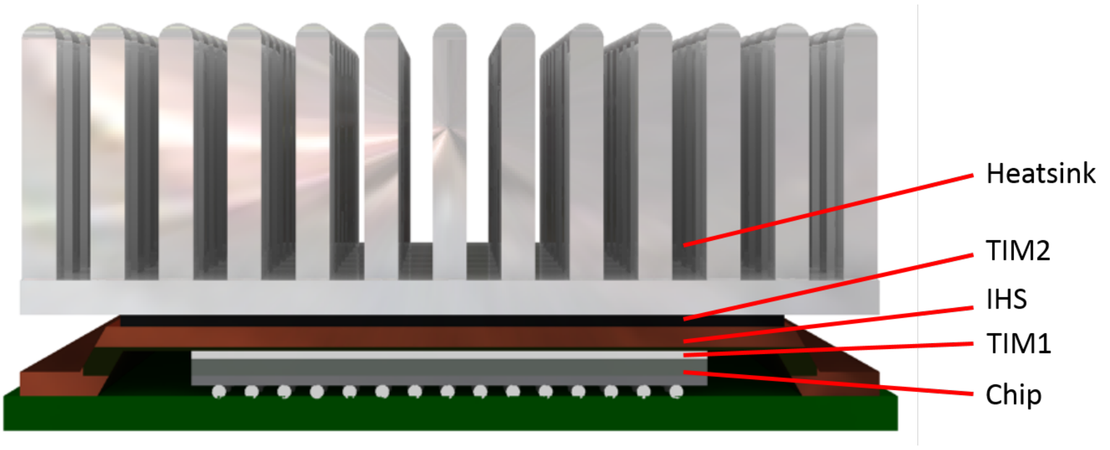

Figure 2.2: A typical BGA package with TIMs between chip and internal heat spreader (IHS), and between IHS and heatsink.

- If the TIM is in liquid or solid form, both when applied and in use. TIMs that are liquid during handling can lead to a somewhat messy process and uncertain BLT, but are generally able to infiltrate voids well if the viscosity is low enough. On the other hand, TIMs that are solid during application, like a pad, are easier to process but might not be able to conform to the substrates as well as liquid TIM.

- During operation, if the TIM is liquid it can be susceptible to pumping out of material from the interface.

- For TIMs that are solid in operation there can be significant stress induced due to difference in coefficient of thermal mismatch (CTE) between the mating surfaces. In this case, the TIM needs to be soft enough to flex and absorb this stress in order to prevent cracking or delamination.

- If the TIM has an adhesive function or if a constant pressure is required during operation.

Depending on application, any and all of these parameters can be important, with different weights. This means that the research into novel TIMs can have a variety of different focuses, not all of them necessarily on the thermal aspect.

Two different applications for TIMs can be seen in figure 2.2. It shows a typical ball grid array (BGA) package with a heat sink, which has two instances of TIM. The first instance is placed between the heat generating chip and the internal heat spreader (IHS), in a TIM1 application. TIMs not placed directly into contact with the heat generating chips are called TIM2, in this case between the IHS and the heat sink.

TIM1 application typically operate at higher temperatures and power densities, and thus have stricter requirements on thermal performance. They also connect a semiconductor on one side with a metal or ceramic on the other, which can have very different CTE (e.g. 3 ppm/K for silicon and 24 ppm/K for aluminum), which

Type	**Thermal conductivity** (W/mK)	**BLT** (μm)	**Thermal interface resistance** (Kmm^2/W)	**Pump-out**	**Absorbs stress**	**Reusable**	**Replaceability**
Thermal grease	0.4 - 4	20-150	10 - 200	Yes	Well	No	Medium
Thermal Pad	0.8-3	200-1000	100-300	No	Well	Yes	Excellent
Phase Change Material	0.7-1.5	20-150	30-70	Yes	Well	No	Medium
Thermal Gel	2-5	75-250	40-80	No	Medium	No	Medium
Thermally Conductive Adhesive	1-2	50-200	15-100	No	Medium	No	Poor
Solder	20-80	25-200	<5	No	Poorly	No	Poor

Table 2.1: Common types of commercial thermal interface materials and typical properties [4–15]

in turn means that TIM1 applications are at risk of reliability issues unless the TIM can absorb the stress.

2.1 Current Thermal Interface Materials

Current commercial TIMs can be divided into several categories, that each have different properties and applications. A summary of the properties of different common TIM types is given in table 2.1.

Thermal grease – Thermal grease consists of thermally conductive filler in a silicone or hydrocarbon oil and has historically been widely used in industry. It conforms well to the substrates and can form thin BLT, leading to thermal interface resistance approaching 10 Kmm^2/W for the highest performing thermal greases[4]. It is also cheap compared to other TIM types, hence its popularity. It is applied as a paste leading to a somewhat messy processing, which is one of the large drawbacks. Since it is in liquid form, it is affected by the pump-out effect, which negatively affects the reliability. Also specifically for thermal grease, the matrix surrounding the fillers preferentially flows out of the interface, leading to a dry-out of the interface.

Thermal Pads – Like thermal grease, thermal pads consist of thermally conductive fillers in a polymer matrix. However, in the case of thermal pads the polymer matrix is heavily cross-linked, leading to a solid pad, which is much easier to handle. This leads to corresponding weaknesses of thick BLT (around 200-1000 μm[5]) and requiring high pressure to properly conform to substrates. To be able to conform to the substrates the softness of the pad is very important, and higher filler fractions of conducting particles increase the stiffness of the composite. However, this will negatively affect the thermal conductivity, the overall performance is severely limited by this trade-off between softness and thermal conductivity.

Phase Change Materials – Phase Change Materials (PCMs) aim to combine the best properties of thermal grease and pads. They consist of a matrix material with a melting temperature between room temperature and operating temperature. This allows them to be handled like a pad, but melts during operation and is able to conform to the substrates and form a thin BLT like thermal grease[7]. It is also possible to have a PCM with a melting temperature above the operating temperature, in which case the TIM is reflowed during processing and kept solid during operation.

Gels – Yet another particle laden polymer type, gel matrices generally consist of silicone polymer which are weakly cross-linked, enabling both liquid and solid behavior[16]. It is dispensed like a liquid, but cured afterwards to form a more solid structure[5], eliminating pump-out, while still keeping a low modulus to absorb stress.

Thermal Conductive Adhesives – Thermal Conductive Adhesives (TCAs) form bonds to both substrates and eliminates the need for external pressure or fastening. Like the above-mentioned TIMs, they consist of a thermally conductive fillers in a polymer matrix, in this case typically epoxy. Like gels, TCAs are generally dispensed as liquids and cures to form a solid joint. TCAs are similar to gels, but are more rigid and provide stronger adhesion between the substrates. Solid versions of TCA also exist, which work as a double-sided tape.

Solders – Solder TIMs are reflowed after application to form metallurgical bonds between substrates. They can be applied either as solder paste or as a preform foil. Since the TIM consists of metal, the inherent thermal conductivity of solder TIM is much larger than polymer based TIMs. Together with liquid form which can fill out voids and wet to substrates during reflow, a very low thermal interface resistance can be achieved[6]. The main concern for solder TIMs is voiding during reflow[17], and the high modulus of solder joints, leading to stress-induced cracking. Also, the cost and complexity in processing is a concern[17].

2.2 Recent Thermal Interface Materials Development

For a large number of applications, it would be beneficial to use TIM with superior or alternative qualities compared to existing TIMs. This has led to large amount of research into new materials and structures that can be used for thermal interfacing. Paper A is a thorough review into the various research avenues of TIMs. In particular, three main categories of TIM which have attracted significant attention have been identified: Particle laden polymers (PLPs), continuous metal phase TIM and carbon nanotube (CNT) array TIM.

2.2.1 Particle Laden Polymers

Particle laden polymers (PLPs) are compounds which consist of filler micro- or nanoparticles inside a polymer matrix. PLP TIMs come in a variety of forms, and can be liquid, solid or cured after application. Most commonly used commercial TIMs fall under this category, such as thermal grease, thermal pads, PCMs, gels, or thermal conductive adhesives. Despite the large variety, from a research perspective they are quite similar, and focus is mainly on the fillers used, their material properties, shapes and filler fraction.

PLPs function by utilizing the polymer matrix to spread, adhere and conform to the mating surfaces. The polymers themselves generally have very low thermal conductivity (< 0.2 W/mK), and for this reason, filler particles with high thermal conductivity are introduced into the matrix in order to conduct the heat. Since the thermal conductivity of the matrix is so low, in order to create an efficient TIM, the heat needs to be able to flow between particles through inter-particle contact

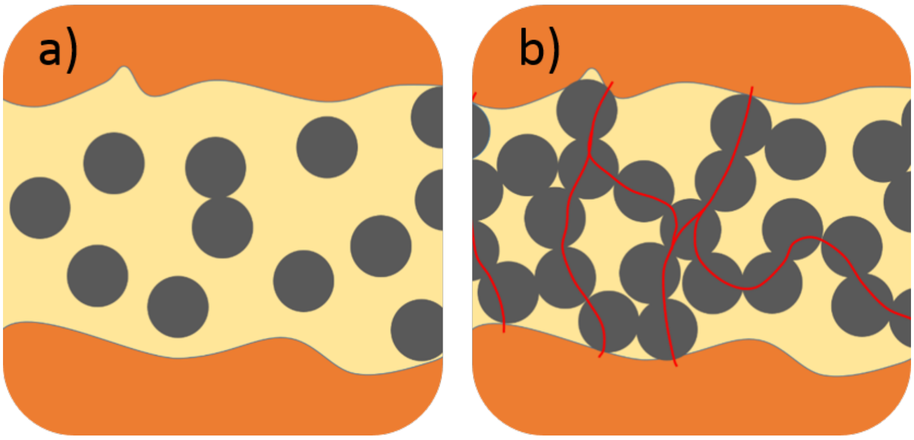

Figure 2.3: Percolation in PLPs. a) Insufficient filler fraction for percolation and thus no continuous heat paths. b) Filler fractions above percolation threshold, and thus continuous heat paths between surfaces.

without going through the matrix. For this, the density of fillers needs to exceed the percolation threshold, as demonstrated in figure 2.3. At the percolation threshold, the composite thermal conductivity sharply increases. Further increase in filler fraction further increase the composite thermal conductivity, although at a continuous pace. Nonetheless, the final thermal conductivity of PLPs is usually much lower than the filler bulk thermal conductivity, and commercial PLP compounds usually range between 1-10 W/mK.

On the other hand, the mechanical properties, especially the viscosity, of the compound is dependent on the filler fraction. Too high filler fraction will cause the compound to become difficult to apply, and may not conform well to the surfaces and therefore cause significant contact resistances. The main goal of the research into PLPs is therefore to achieve as high thermal conductivity as possible at a sufficiently lower filler fraction.

As mentioned before, the most important figure of merit is the thermal interface resistance according to equation 2.1. However, in the case of PLPs, most reports only mention a value for the thermal conductivity, without any actual measurements of a TIM application. For this reason, the thermal conductivity and filler fraction are the comparative figures of merit for this section.

Filler materials

The filler particles in PLPs can consist of a number of different materials. A list of materials encountered within this study can be seen in table 2.2, together with their respective bulk thermal conductivity. Within these materials, three groups can be distinguished: ceramics, metals and carbon allotropes.

Ceramic materials are electrically insulating, which can be important for many applications. Out of the ceramics, BN has the highest thermal conductivity, and even higher thermal conductivity has been reported for very thin sheets, making it an increasingly interesting material for thermal management applications. As early as 1998 Ishida et al.[18] reported a thermal conductivity value of 32.5 W/mK for BN

Material	Conductivity (W/mK)
Graphene	6000
SWCNT	3500
MWCNT	3000
Graphite	100-400 (in-plane)
BN	250-300
Ag	427
Cu	393
Au	315
Al	237
AlN	170
Al_2O_3	39

Table 2.2: Thermal conductivity of common types of fillers

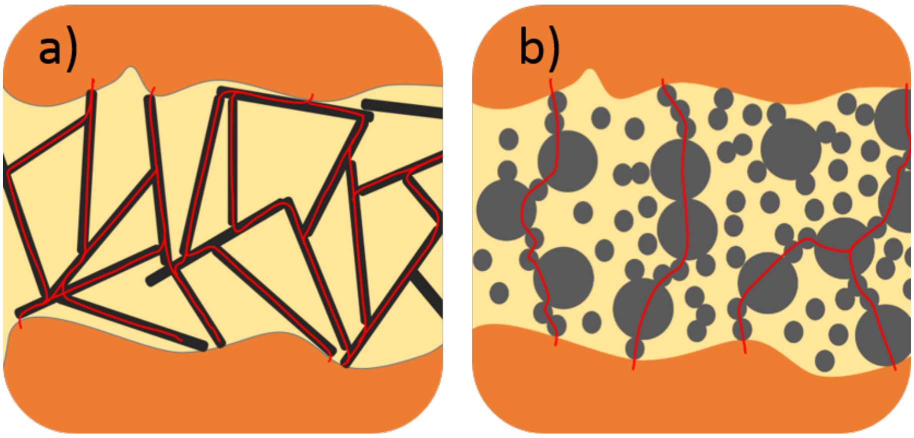

Figure 2.4: Filler combinations to achieve percolation at lower filler fractions. a) High aspect ratio fillers. b) Bimodal particle size distribution.

filled polybenzoaxine which still stand as the highest value to date, although at a very high filler fraction (88 wt%). It has more recently been investigated further in silicone thermal pads[19], epoxy[20, 21] and other polymer matrices[22, 23]. Another ceramic which has attracted academic interest is AlN[24, 25], which is also together with Al_2O_3 popular in commercial applications.

Carbon allotropes come in many forms, such as diamond, graphite, CNTs or graphene. Out of these, CNTs and graphene stand out due to their potentially incredible thermal conductivity [26–28]. Another interesting property is the 1D and 2D nature of these materials respectively. By using fillers with a high aspect ratio, it is possible to achieve percolation at much lower filler fractions than by using spherical fillers, as seen in figure 2.4a. For CNTs, percolation has been achieved at filler fractions as low as 0.1-0.2 wt% [29, 30].

However, there is a very high thermal contact resistance between CNT and matrix [31–34], as well as phonon dampening due to their interaction [35]. The thermal conductivity improvement of PLPs with CNTs is quite modest, and much lower than what would be expected from a rule of mixtures [36].

However, unlike CNTs, graphene and graphite flakes has been shown to increase the thermal conductivity of epoxy by about 20-30 times at 20-30 wt%[37–41] filler fraction. The thermal conductivity improvements in graphene/graphite composites are much higher than for CNTs, even at the same filler fraction[42], as well as significantly cheaper and easier to manufacture.

Metals have very high intrinsic bulk thermal conductivity and good handling properties. The best commercially available thermal greases have a thermal conductivity of about 8 W/mK with a filler of Ag flakes. Most recent progress using metal fillers are focused on using metal nanowires (NWs) rather than spherical fillers. Similarly to CNTs, metal nanowires can, due to their 1-D shape, form percolating networks at very low filler fractions.

Ag is the most popular metallic filler in commercial compounds and is a natural candidate, and has been demonstrated as TIM filler by electrodeposition of a template[43, 44] or a chemical process[45, 46]. The electrodeposition method forms a highly aligned network, which allows for a significantly higher thermal conductivity than using a random dispersion, 30.3 W/mK [44] compared to 1.4 W/mK[46]. In addition to these methods, Pashayi et al. demonstrated a self-structured metallic nanowire network based on agglomeration and sintering of PVP-coated Ag-nanoparticles which exhibits a thermal conductivity of up to 38.5 W/mK at 48 vol%[47, 48].

Other metals have also been investigated. Wang et al. found that CuNWs gave a larger conductivity enhancement at a lower filler fraction than AgNWs, and achieved a thermal conductivity of 2.46 W/mK at a low filler fraction of 0.9 wt%[46]. Nanowires of Ni[49, 50] and Au[51] have also been investigated.

Filler combinations

A method of increasing the thermal conductivity at a lower filler fractions is to combine different fillers into the same TIM matrix. Different fillers create synergistic effects that increases the effective thermal conductivity beyond what would be expected from models. The most common mechanisms behind the synergistic effects are size variations and variations in aspect ratio of fillers. Size variation can help forming percolating networks (see figure 2.4 b) and improve packing ratio[23, 38, 52]. Variations in aspect ratio can combine the percolation-forming networks formed by high aspect ratio fillers with the bulk thermal transport properties of bulk and 2D fillers[53].

Filler combinations reported typically includes filler materials with different dimensionality (1D, 2D or 3D). Lee et.al. demonstrated the concept of mixing 1D rods with spherical particles[54] in 2006. Recent progress includes studies of Boron Nitride (BN)/CNTs[55–57], BN/CNFs[58] and graphene oxide (GO)/CNT[59, 60] hybrid composites, which all combine 1D and 2D fillers, which are more effective for creating conducting networks than 1D/spherical filler combination[56].

Since spherical 3D and 2D flake fillers already exist as commercial compounds, the addition of a high aspect ratio filler into commercial thermal grease has proven

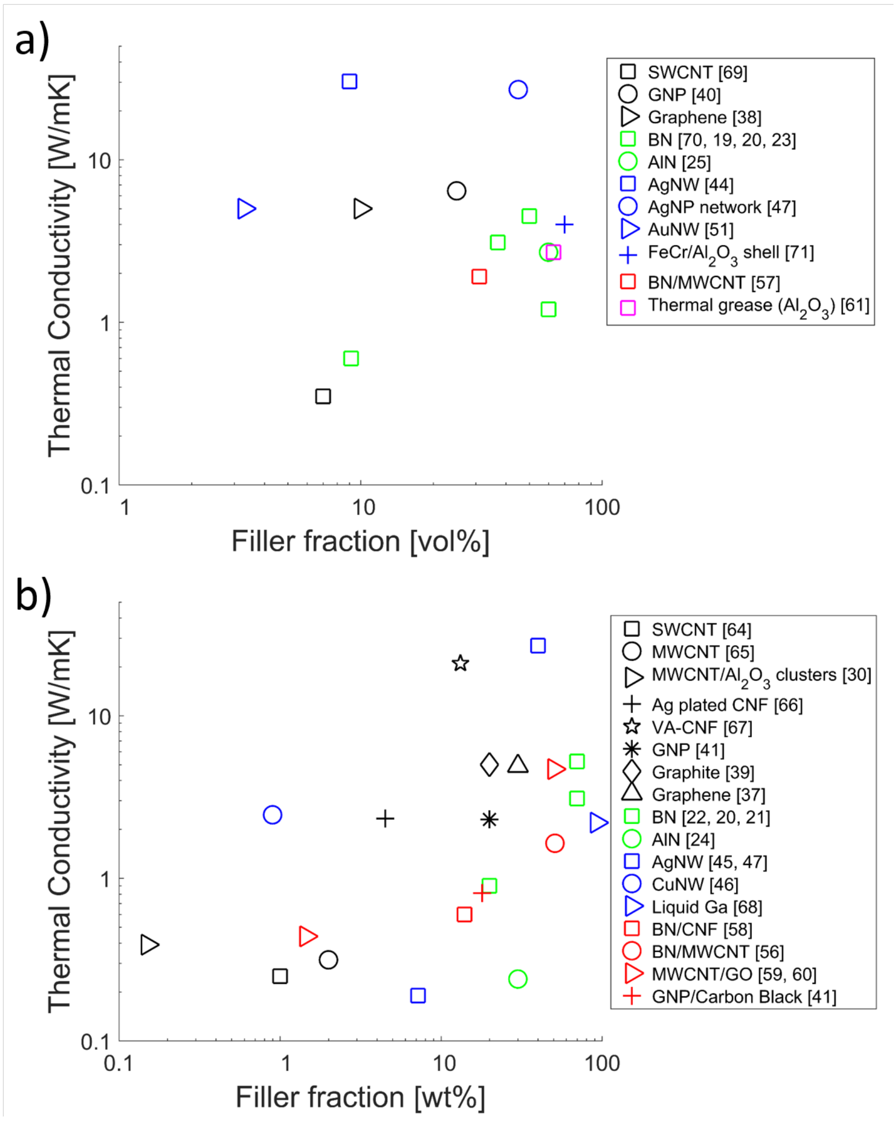

Figure 2.5: Thermal conductivity as a function of filler fraction for various PLPs, colored based on different categories of fillers: carbon allotropes (black), ceramics (green), metal (blue), hybrid fillers (red) and a commercial compound (pink). The data is divided into two graphs depending on whether the filler fraction is measured in volume or weight percentage.

a popular method of investigating the synergistic effects of spherical/high aspect ratio hybrid fillers[38, 61–63]. Among these the highest thermal conductivity value reported to date is 14 W/mK by the addition of an optimized mixture of graphene and multi-layer graphene into thermal grease at a low filler fraction of 2 vol%[38]. Also, the addition of MWCNTs to thermal grease has been directly shown to decrease the temperature of a running microprocessor[63].

Conclusion

A summary of recent reports on PLPs can be seen in figure 2.5, including some reports not otherwise discussed in this thesis [58, 64–71]. The thermal conductivity of the presented compound is plotted against total filler fraction. The figure is split into two graphs as filler fraction value reported is alternatively given in volume fraction or weight fraction. The volume fractions give a more accurate representation of the effect of higher filler fractions, but general trends can be distinguished in both cases.

It is clear that alignment of high-aspect ratio fillers such as carbon nanofibers and metal nanowires can provide a magnitude higher thermal conductivity at the same filler fraction compared to unaligned fillers, and is generally the only way to increase the thermal conductivity beyond 10 W/mK. Also noteworthy is that although CNTs have shown rather unimpressive performance as fillers, other carbon allotropes such as graphene and GNP have shown better performance than other kinds of fillers at similar fractions.

Aside from these few exceptions, the actual performance of PLPs has not increased significantly during the last decade, and recent reports have similar performance to commonly available industrial TIMs. Despite this, the research area of PLPs has seen a relatively large amount of publications. A possible explanation is that it is relatively easy experimentally to test new fillers or mix together a new combination, even though the end result is rarely groundbreaking. Further evidence of this is that there are few publications on PLPs in high impact journals compared to the other categories.

The current industry is dominated by PLPs in different varieties, and there is a large infrastructure already in place for developing new compounds. This means that any breakthrough in research has the potential to quickly reach the market. The matrix material has little effect on the thermal conductivity, allowing filler development to have an effect on a wide range of TIMs.

2.2.2 Continuous Metal Phase TIM

Solder based thermal interface materials are used in industry in applications where a low thermal interface resistance is critical. Solder is the only commercially available TIM which can provide low thermal interface resistances of <5 Kmm^2/W, due to the inherently high thermal conductivity of metals, and the reflow process which largely eliminates voids and forms metallurgical bonds. Solders can be applied either as solder paste or as a thin foil sheet with or without flux. It provides a continuous metal phase for heat transfer at a high thermal conductivity, nearly eliminating internal interface resistance. However, their rigid structure can lead to poor stress absorption further leading to cracking during thermal cycling due to CTE mismatch. As such, research on metal TIM tends to focus on decreasing modulus or otherwise improve the reliability of the TIM, rather than further thermal interface resistance improvements.

Historically, the most widely used solder alloy is tin-lead (SnPb), however due to the toxicity of lead, their use is now mostly forbidden in the European Union[72]. This presents a challenge for both traditional soldering and solder based TIMs, as lead free solders typically have higher melting points, modulus and are more brittle than SnPb solder[73]. The development to find better replacements are ongoing, and for research into TIMs based on solders it is important to have an overview of this research field as well. Kotadia et al.[74] have recently provided an extensive and up to date review article for this purpose.

The most common solder to be used in thermal interface applications in industry today is indium. It is a comparatively soft metal, allowing it to conform to substrates and absorb stress, and has a relatively low melting temperature of 157°C. Both AMD[75] and Intel[76] have developed and used indium as TIM in TIM1-applications for high-end processors. On the other hand, Indium is a relatively rare metal with a high price and limited supply[77]. There is a drive away from indium dependency, and therefore alternative alloys are also under being investigated, such as Sn-Ag-Cu (SAC) [78] and Sn-Bi [79].

Solders are typically solid in operation, but there are alloys with very low melting temperature (LMAs), such as Ga, Ga-In and In-Bi-Sn with melting points at 30°C, 16°C and 60°C respectively. These alloys can be used as TIM, and melt during operation, which allows for simultaneous mechanical decoupling and wetting, resulting in a very low thermal interface resistance [80–82]. However, LMA TIMs are susceptible to material pumping out of the interface, Ga containing alloys are corrosive to must substrates [83], and In-Bi-Sn has a rapid growth of brittle intermetallic compounds at the surfaces [81].

Metal TIMs are usually limited to alloys with a melting temperature low enough to prevent damage to components, which usually excludes any alloy with a melting temperature above that of the solder used for the electronics assembly. However, higher melting point materials can be used in the form of nanoparticles (NPs) which sinter together at a much lower temperature than the melting point. This has been demonstrated with AgNPs, which can achieve a thermal interface resistance of less than 1 $\mathrm{Kmm^2/W}$ [84].

Metal matrix composites

One of the most interesting avenues for potential breakthrough technologies is the research into novel nanostructured composite materials. A combination of different materials can, through careful structuring of the components at small scales, combine the best thermal and mechanical properties of the different constituents. Since solder has an unmatched thermal performance, the use of solder alloys as a matrix material in a composite is attractive. By combining the solder matrix with fillers or other nanostructures the mechanical properties can be significantly enhanced while retaining the high thermal conductivity of the solder.

One such composite consists of bulk solder in a liquid phase sintered solder composite material [85]. High-melting phase material such as Sn or Cu was embedded in a matrix of a low-melting phase such as In. The resulting composite combines the attractive properties of In, such as melting point and low shear strength, with the compressive creep strength and price of Sn or Cu [85, 86]. Surface modification of Cu particles to prevent IMC formation created a composite with high mechanical

Description	R_{th} (Kmm^2/W)	BLT (μm)	Reference
In-Bi-Sn	3	<30	[81]
Gallium	2.6	3	[80]
Sn-Bi solder paste	5	50	[79]
Liquid Phase Sintered Sn-In Composite	21	25	[85]
Liquid Phase Sintered Cu-In Composite	2.1	100	[87]
Sintered AgNP (250°C)	2	10	[84]
Aligned Graphite Solder Composite	3.5	200	[62]
Solder Graphite Network Composite	3.8	50	[95]
SAC-Polymer Fiber Composite	2-4	35-65	[97]
SAC-Carbon Fiber Composite	2-7	65-160	[98]

Table 2.3: Summary of recent continuous metal phase TIM progress

strength and a thermal interface resistance of 2.1 Kmm^2/W [87]. Modeling further suggests that the composite may be improved further by disc-shaped inclusions instead of spherical particles [88].

Raj et al. demonstrated a concept of coelectrodeposition of metal films with filler particles incorporated [89], using SiC and graphite fillers in a Sn matrix. A similar concept was used by Nagabandi et al., wherein functionalized boron nitride nanosheets were included into an Ag matrix [90]. They showed a composite with a thermal conductivity of over 80% of that of pure Ag, together with a significantly reduced modulus.

Alternatively fillers can be mixed with solder paste to produce the composite after reflow which has been reported with fillers of CNTs [91], graphite [92], Zn [93] and Cu [94] into various solders. Despite some successful results in increasing creep resistance [92, 94] and reducing CTE [91] and IMC formation [93], there has been no TIM applications reported until recently, when Sharma et al. [95] demonstrated a solder-graphite network composite. Graphite forms a self-assembling network through mechanical compression, after which a flux-less reflow forms a network in the solder matrix. The resulting composite provides thermal resistance as low as 1.4 Kmm^2/W at 0.92 MPa and a CTE of 10 ppm/K.

As an alternative to a self-assembling composite, Chen et al.[96] proposed a vertically aligned solder-graphite sheet composite in which alternating vertically aligned graphite sheets and solder forms a composite. By varying the amount of solder to graphite the CTE of the composite can be controlled directly. Finally, another top-down approach on metal matrix composite fabrication is the solder matrix fiber composite (SMFC) which is discussed in detail in chapter 3.

Outlook

Table 2.3 shows recent results on continuous metal phase TIMs. The thermal interface resistance is very consistent in the 2-5 Kmm^2/W range owing to the high thermal

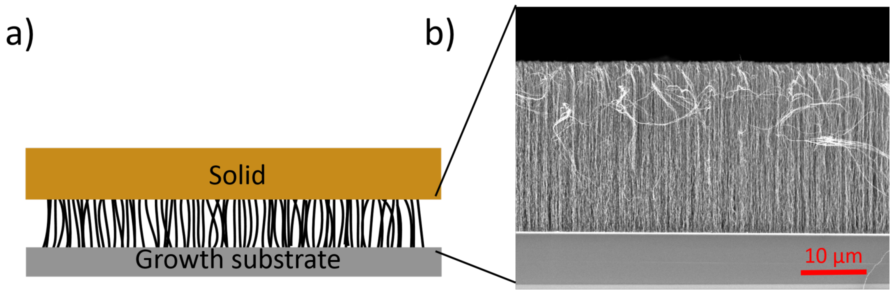

Figure 2.6: a) Schematic of a CNT array TIM. b) Scanning electron microscopy (SEM) image of a CVD grown CNT array.

conductivity of metals and excellent compliancy after reflow. The challenge is still to increase the reliability through improving mechanical properties.

Solders already have widespread industrial applications and is a very mature research field. As such, the path from new research to applications is, as with PLPs, relatively short. Much research is based on small incremental changes upon existing technology, where application and a large part of the manufacturing methods are already established. In addition, since solders are the sole currently existing alternative for high-performance TIMs, improvements would be relatively easy for industry to adopt compared with completely novel types of TIMs.

2.2.3 Carbon Nanotube Arrays

Instead of using CNTs as fillers in PLPs, having an array of CNTs that individually span the whole BLT, as seen in figure 2.6, would completely eliminate the internal resistances. Such a CNT array could therefore be a practical way of harnessing the high thermal performance of CNTs in a TIM application [99]. Vertically aligned CNTs are grown by a chemical vapor deposition (CVD) process and pressed against an opposing surface. The mechanisms for CNT CVD is based on the thermal breakdown of a hydrocarbon gas in the presence of a metal catalyst particle [100]. The carbon then precipitates and crystallizes into a CNT that grows from the catalyst particle. With a high enough density of CNTs, geometrical constraints from neighbours will then align the CNTs vertically, forming an aligned array.

In a TIM application, the CNTs act like small springs, which bends and conforms to the surface. Additionally, each CNT would be independent in the x-y plane, allowing the array to easily absorb any CTE mismatch between the two surfaces and completely avoid the large drawback of metal based TIMs.

The thermal conductivity of a carbon nanotube can reach as high as 3000 W/mK [27, 28], but the bulk value for CNT arrays is much lower, both due to low CNT density, defects and imperfections in the CNTs themselves [101]. A typical value for a CNT array is on the order of 10 W/mK [101]. While there is a large discrepancy between measured and theoretical thermal conductivity values, at moderate bond lines (<30 μm) the thermal conductivity will have relatively low effect on the thermal interface resistance compared to the contact resistances [102–104]. For instance, B. Cola et al. [105] measured the thermal interface resistance components for a

Si-CNT-Ag interface at 0.241 MPa using a photoacoustic method, and while the contact resistance was found to be 1.7 Kmm^2/W at the Si-CNT and 14 Kmm^2/W at the CNT-Ag interface, the thermal resistance from the bulk CNT array was less than 0.1 Kmm^2/W.

The dominance of the contact resistance, especially at the attached surface, on the overall thermal interface resistance can mostly be explained by a limited number of the CNTs in actual contact to the opposing substrate [104, 106]. There is little conduction between adjacent CNTs in the array, and so only the fraction of CNTs in contact with both sides can significantly contribute to the heat transfer. Additionally, the intrinsic contact resistance (Kapitza resistance) between CNTs and metals is significant[107].

As shown by Cola et al., the bulk thermal conductivity of the CNT array has relatively little effect on the overall thermal interface resistance. However, the geometrical and mechanical properties of the CNT array are still important, and multiple studies have confirmed that the CVD growth parameters of the CNT array greatly affects the resulting TIM [108–111]. In particular the compliance of the CNT array is a dominant parameter, with lower modulus allowing more CNTs in effective contact with opposing substrate.

Bonding of CNT arrays

Since the largest contributor the thermal interface resistance of CNT array TIM is the contact between the tip of the CNT array and the opposing surface, much research has been focused on reducing this contact resistance by bonding the surface to the tips. The goal is two-fold: increasing the number of CNTs in contact with the surface, and reducing the Kapitza resistance at individual CNT tips. Typically this is done by using an additional layer which partly penetrates into the CNT array to come into contact with additional CNTs.

An established method for bonding materials together is metal bonding, using metals as the intermediate layer. Tong et al.[103] demonstrated a bonding approach using a In solder layer at the free CNT ends, which partly penetrates the array and contacts a larger fraction of CNT. This results in a decrease in the total thermal interface resistance of an order of magnitude, down to 1.7 Kmm^2/W. Other metal bonding methods include metallization of Ti/Au onto both CNT array and bonding surface, which bonds at 220°C due to Au-Au self-diffusion[112], and palladium thiolate used to coat the sidewalls of CNTs with Pd nanoparticles[113], forming a Pd weld after baking at 250°C.

To avoid increased bonding temperatures, Barako et al.[114] proposed a bonding solution in which a Sn-coated foil comprised of many thin layers of alternating Au and Ni is used as a bonding layer. A pulsed electrical current initiates an exothermic reaction to alloy the layers into $Au_{0.5}Ni_{0.5}$, which locally heats up the foil enough to melt the Sn layer to the CNT array.

While metal bonding has shown significant improvements in thermal performance, it does nothing to address the large Kapitza resistance at the CNT-metal interface. For this reason, progress has been made towards non-metal bonding of CNT arrays

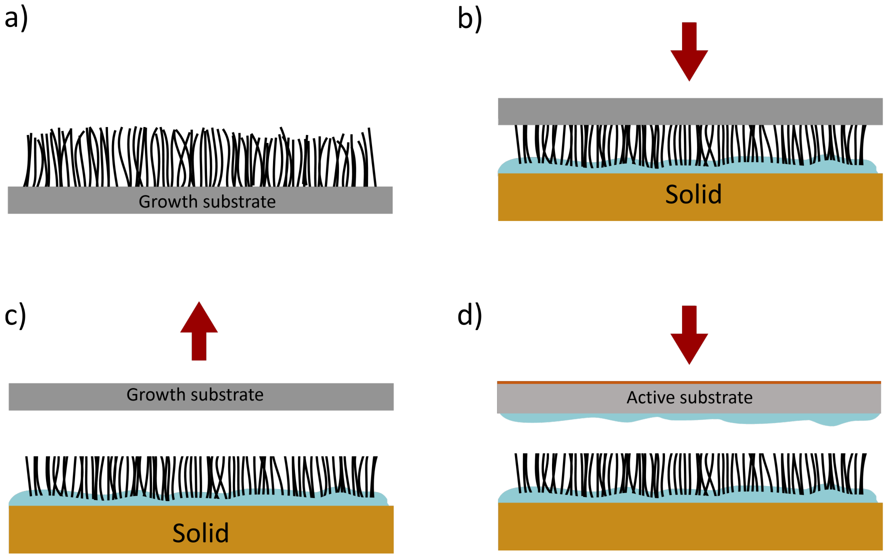

Figure 2.7: Bonding and transfer process for a CNT array TIM. a) CNT array is grown on a sacrificial silicon chip. b) The array is bonded to another substrate. c) The sacrificial silicon chip is peeled off. d) A new active silicon chip can be attached instead.

using polymer coatings[115–117] or chemical functionalization[118–120]. Polymer bonding can serve to increase real contact area, as demonstrated using a spray on polymer coating together with a solvent, which pull CNTs into contact using capillary forces[116]. In addition, chemical functionalization, either directly or in conjunction with a polymer coating can create bonds between CNTs and substrate, greatly reducing the thermal contact resistance.

Ni et al.[115] introduced an azide polymer based thermal glue which also bonds covalently with CNTs through C-N bonds, achieving a low thermal interface resistance of 1.40 $\mathrm{Kmm^2/W}$. They further suggests that bonding with an element lighter than carbon gives lower contact resistance due to higher vibrating frequencies. Kaur et al.[119] also managed a six-fold reduction of the thermal resistance at CNT-Al and CNT-Au interfaces using covalent bonding of short organic molecules, also bonding to CNTs with a covalent C-N bond. Taphouse et al.[120] showed a similar reduction of thermal resistance using a pyrenylpropyl-phosphonic acid surface modifier to bond CNT arrays to metal oxide substrates, although this bonds to CNTs using $\pi - \pi$ bonds rather than covalent bonds.

Transfer of CNT arrays

While CNT array bonding can reduce the thermal resistance of the interface, there is a fundamental problem to overcome before CNT arrays can be commercially viable. In a majority of studies, the CNT array is synthesized directly on the silicon chip which is to be cooled. However, the CVD process require high temperature, typically at least 700°C, which is incompatible with modern CMOS electronics (max 500°C). There has been some effort into optimizing a low temperature CVD process [100, 109], but so far it has proven challenging to synthesize CNT arrays of sufficient quality at low enough temperatures. Another option is to grow the CNTs on the heat sink side, and this has been demonstrated on both Cu [121] and Al [122, 123].

However, the most promising alternative appears to be the transfer of the CNT array from a sacrificial growth substrate into the interface. A bonding method as discussed in the previous section can be used to attach the array onto one surface. Then, the original growth substrate can be peeled off, and the other mating surface can be attached. An illustration of this is seen in figure 2.7

Transfer has been demonstrated for solder[124, 125], metallization[112] and thermocompression[126, 127] bonding. Despite bonding, the thermal contact resistance of the growth substrate/CNT array interface is an order of magnitude lower than at the bonding interface, and a corresponding increase in thermal interface resistance is seen after transfer compared to just bonding the free ends[112].

A more flexible alternative to transfer of bonded CNT arrays is to grow CNTs directly on both sides of a thin foil[128–130]. This allows to TIM to be applied anywhere in the same manner as a thermal pad. While the arrangement is in principle equal to two conventional CNT array TIMs, in reality the foil can conform to the substrates, increasing the fraction of CNT contacts on both sides. Cola et al. achieved thermal interface resistance less than 10 $\mathrm{Kmm^2/W}$ at moderate pressures[128], on par with single-sided CNT array TIMs, suggesting that the added conformability and real contact outweighs the higher number of interfaces.

Another way to create a freestanding film that can be applied as a thermal pad is to infiltrate the CNT array with a polymer, forming a composite material which can easily be applied. Several investigations into CNT array polymer composites have been conducted, both as freestanding films [131–133] and attached to original substrate [34, 134]. However, in each case the thermal conductivity of the composite is lower than for a naked array. Proposed explanations are polymer preventing some CNTs to contact with a substrate, decreased alignment due to processing and damping of phonon modes in the CNTs by the polymer matrix[132].

Outlook

Research done on CNT array TIMs is summarized in figure 2.8, which shows the reported thermal interface resistance values versus total CNT array height [135–139]. The correlation between thermal interface resistance and CNT array height is very weak, which is consistent with performance limited by contacts between CNT array and substrates. The importance of a good bonding is apparent, and further research should continue to investigate the possibilities of a facile, scalable bonding method.

The main limitation preventing widespread industrial use of CNT array TIMs is the production capacity of CNT arrays, which is currently lacking scale and process controllability. While production of randomly aligned CNTs are starting to reach industrial scale[100], growing a uniform vertically aligned CNT array poses additional limitations on scaling. For an introduction of commercial CNT array TIMs the CVD process has to be improved and scaled up significantly. Roll-to-roll CVD systems for

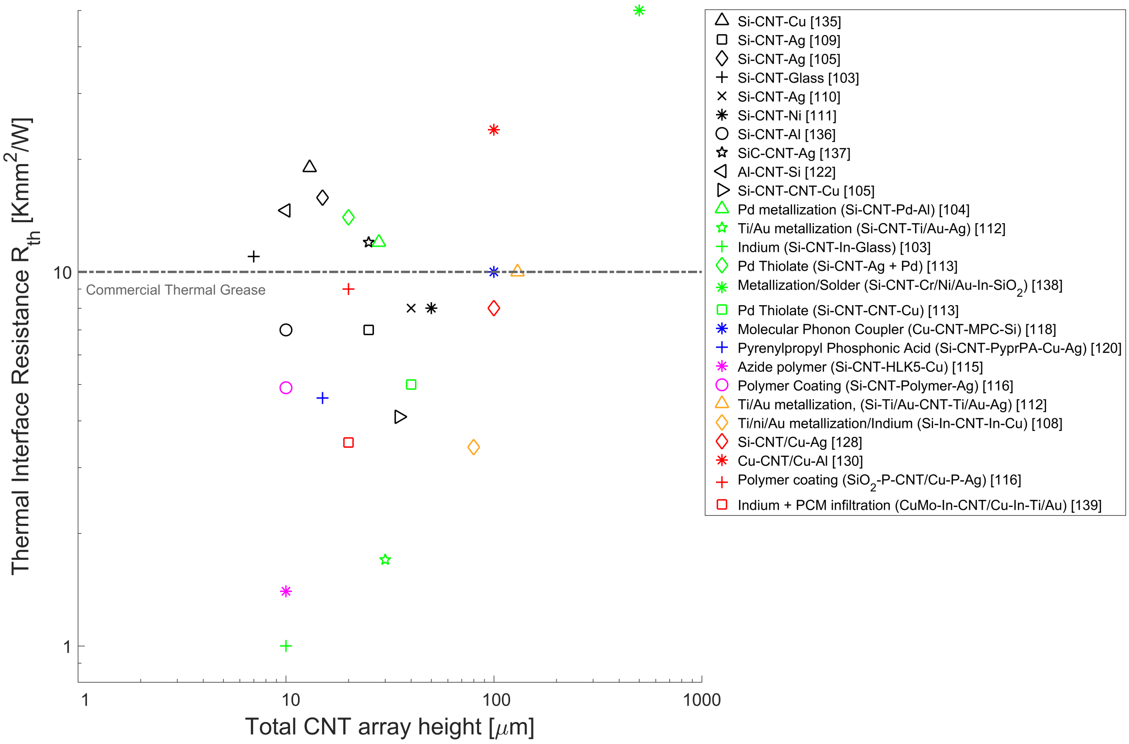

Figure 2.8: Summary of CNT array TIM results, plotted as thermal interface resistance versus CNT array height. The results are divided into different categories: bare CNT arrays (black), Metal bonded CNT arrays (green), chemically bonded CNT arrays (blue), polymer bonded CNT arrays (magenta), transferred CNT arrays (orange) and double sided CNT array foils (red). Dashed line represents the thermal interface resistance of the best available thermal greases, at 10 Kmm^2/W.

graphene[140] and CNT[141] production have recently been demonstrated, which could potentially increase volume, although controlling the process remains an issue.

In addition to the manufacturing issues, unlike for PLPs and solder TIM, there is little research on the reliability of interfaces with CNT arrays. Theoretically, the mechanical decoupling of surfaces that CNT arrays allows for should result in excellent mechanical properties, but there is a lack of experimental studies to corroborate this.

2.2.4 Other Novel Concepts

In addition to the previous categories of TIM research, there are a number of novel concepts which have been proposed. These can be divided into three additional smaller categories: mechanically deformed metal, thermally conductive polymer and carbon based TIM.

Unlike continuous metal phase TIM, a mechanically deformed metal does not use melting of the metal to create metallurgical bonds. Rather, in this category, the metal is textured in such a way that mechanical pressure allows it to bend and conform to the surfaces. This has been demonstrated for microtextured metal foils [142–144], tin [145]and copper [146] nanowire arrays and copper nanosprings [147].

The metal nanowire arrays could potentially combine the thermal stress absorption of CNT arrays with the low contact resistance associated with continuous metal phase TIM, if bonded with solder at the interface. This was demonstrated with copper nanosprings for a low thermal interface resistance of 1 $\mathrm{Kmm^2/W}$.

The second category, thermally conductive polymers, utilize the recent discovery that polymers can be modified by increasing crystallinity and alignment of crystallites and chain orientation to increase the thermal conductivity by several orders of magnitude [148, 149]. A polymer nanofiber array was found to be applicable similarly to CNT array TIM with a thermal interface resistance of 12.8 $\mathrm{Kmm^2/W}$.

The third category is that of carbon based TIM aside from CNT array TIMs. The exceptional thermal properties of graphene-like structures can be harnessed in other ways than just CNT arrays and fillers in PLPs. The challenge is to create macroscale 3D structures out of what originates as 1D or 2D (CNT and graphene respectively). One way of creating such a 3D structure out of graphene is to deposit graphene on the surface of a highly porous template, and then selectively etch away the template. Left will be a freestanding graphene foam structure. Zhang et al. demonstrated the possibility of such a graphene foam as TIM, and found that the structure is exceptionally compliant and could achieve a thermal interface resistance as low as 4 $\mathrm{Kmm^2/W}$ at a contact pressure of only 0.1 MPa [150]. A similar foam like structure has also been created by a self-assembled method through a hydrothermal reduction of a graphene oxide (GO) dispersion [151].

Alternatively, instead of a random foam network, a more deliberate alignment can be done. Films of graphite or reduced GO can have a very high degree of alignment and a thermal conductivity in excess of 1600 W/mK [152]. However, this alignment is in the in-plane direction, orthogonal to the heat flow in a TIM application. If graphene sheets could be efficiently aligned in the z-direction instead, it could potentially provide a good TIM candidate. Direct stacking of multiple graphene films has been demonstrated to some success [153], but a more efficient way of aligning the graphene sheets is needed for a practically usable TIM.

Finally, graphene is only the first out of many possible 2D materials, and the attractive properties of graphene could very well be found in other materials as well. One such interesting material is hexagonal boron nitride (h-BN), which has a similar structure to graphene and also high thermal conductivity. However, unlike graphene, it is electrically insulating, which may be important in certain applications. It has already been used as conducting fillers in polymers, both in the form of platelets[22], nanotubes[154], and as a BN foam[155], echoing the use of graphene while retaining its insulating properties.

2.2.5 Summary

Figure 2.9 shows the thermal interface resistance versus BLT from all reports treated within this review where such data could be obtained, including some reports not previously mentioned [156–159]. A few commercial compounds are also included as reference[139, 160]. It contains selected reports in which thermal interface resistance measurements have been done at a given BLT. While not exhaustive, it gives

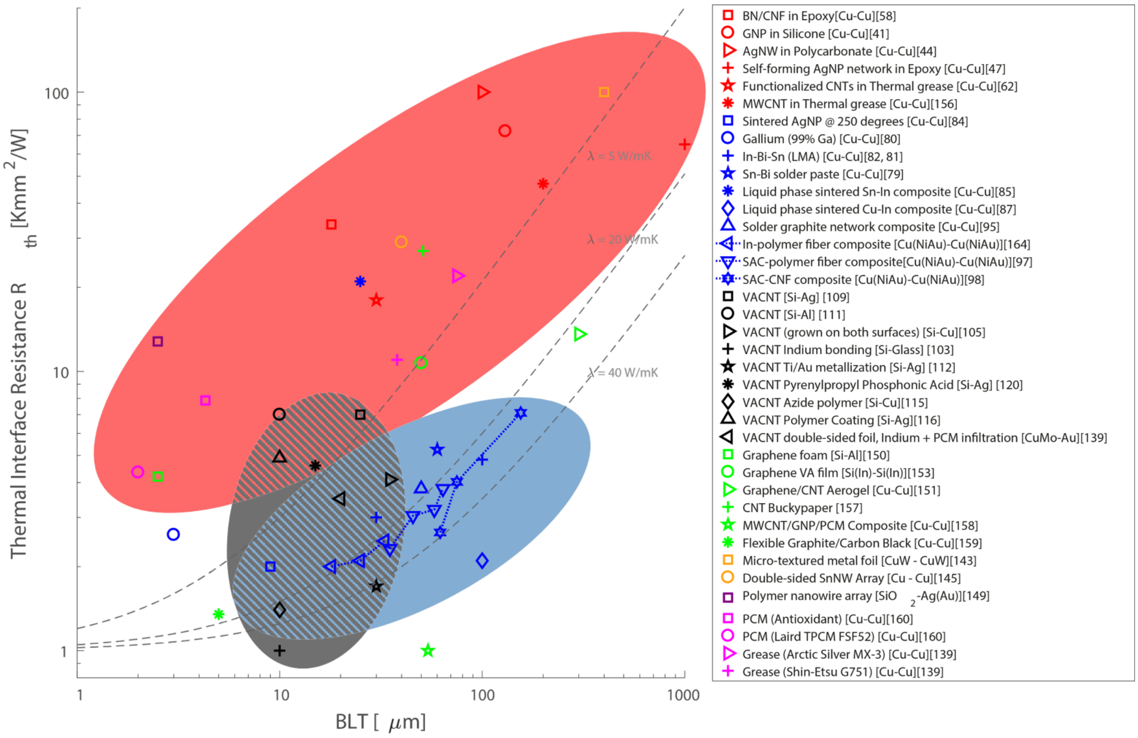

Figure 2.9: Thermal Interface Resistance versus Bond Line Thickness for recent results, based on different categories: Particle Laden Polymers (red), Carbon Nanotube array TIMs (black), continuous metal phase TIMs (blue), other carbon based TIMs (green), mechanically compliant metal TIMs (orange), polymer nanowire array (purple) and commercial TIM references (pink). References for TIMs with a thermal contact resistance of 1 Kmm^2/W and a thermal conductivity of respectively 5, 20 and 40 W/mK are also plotted (dashed grey). The colored ellipses show the approximate region in which the different categories of TIM are found.

an overview of the field in its entirety, and some general trends can clearly be distinguished, as seen from the colored ellipses. Particle laden polymers, despite attracting much interest, has still not improved significantly over the last decade in terms of thermal performance. Indeed, where comparable the performance of commercial thermal grease actually performs better than newer compounds. Metal nanowire filler is a potential breakthrough technology, but as can be seen, despite a very high thermal conductivity, the thermal interface resistance is still very high due to high contact resistance and large BLTs.

Reports on continuous metal phase TIMs all follow a similar relationship between BLT and resistance. Which is consistent with the idea that research within this area is more focused on mechanical properties rather than thermal performance, and actual progress in that area will not be represented in this type of comparison.

As previously discussed, CNT array TIMs perform slightly worse than solders with dry contact, and on par or even better when bonded to a substrate. There is no clear relationship between BLT and thermal interface resistance, which is consistent with the resistance being dominated by contact resistances at the edge of the CNT arrays. It is clear that performance is not the factor limiting CNT array TIMs from becoming commercially available. Nonetheless, CNT array TIM is the most promising new breakthrough technology to enter commercial markets within the relatively near future.

These categories, together with the previously mentioned other novel concepts, build up a picture of the total status of the field.

Chapter 3

Solder Matrix Fiber Composites

3.1 Introduction

The most common use of Solder is to attach components on a PCB and to form electrical connections between them. However, the same properties and technologies that enable excellent electrical connections, also creates good thermal connections.

Due to their ability to form metallurgical bonds towards other metal surfaces together with their high thermal conductivity, solders have been widely used in TIM applications, and is the only commercially available alternative when thermal interface resistances of < 5 Kmm^2/W is required. However, as explained in section 2.2.2, solders can have significant drawbacks in terms of reliability due to a high elastic modulus and rigid structure. This issue is exacerbated as the size of the interface increases, as the strain due to CTE mismatch between the two surfaces is larger. In addition, solder can be difficult to handle during reflow, causing uneven and/or to thin BLT.

As a potential way to address these issues, the solder matrix fiber composite (SMFC) concept was introduced by Carlberg et al. in 2008 [161]. The concept consists of a randomly aligned network of fibers inside a metal matrix as seen in

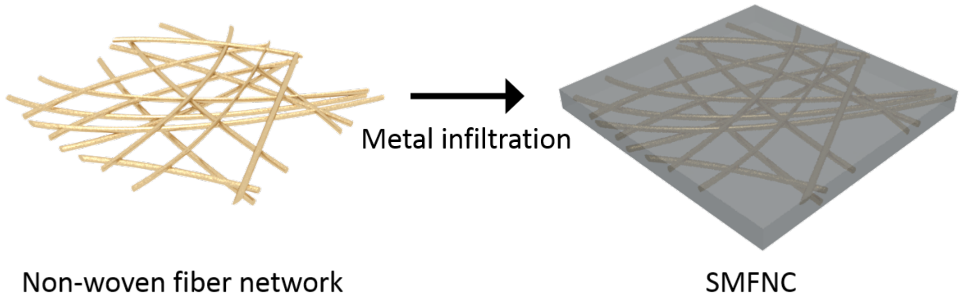

Figure 3.1: SMFC concept, consisting of a non-woven fiber network which is infiltrated with molten metal to form a composite structure.

figure 3.1. The metal part of the composite acts as the solder in normal solder TIM. The fiber network is highly porous, which allows the metal to form continuous heat paths through the TIM. This allows for a high total thermal conductivity despite the presence of a fiber network, which is not necessarily a good thermal conductor. The end result is a composite material which has very similar thermal properties as regular solder TIM.

The fiber network on the other hand, serves several purposes:

- To tailor the mechanical properties of the TIM. Depending on fiber composition the fiber can serve to make the material softer or stronger.
- To prevent crack propagation through the metal phase.
- To act as a spacer during reflow, in order to establish a well-defined and uniform BLT and prevent metal from escaping the interface during molten state.

Both metal matrix and fiber network can consist of a number of different materials. The metal matrix could be any suitable alloy, depending on the requirements for each application in terms of thermal properties, temperature and surface metallization. SMFCs have been demonstrated with In [162–165], Sn-Ag-Cu (SAC) alloys [97, 98] and In-Bi-Sn [161] as metal matrix component. The fiber network can consist of any material available as a non-woven fiber network, depending on desired end properties. So far, the concept has been demonstrated using fibers made out of Ag coated polyimide[97, 164, 165], Carbon Nanofibers[98] and BN[162].

All previous reports have relied on the electrospinning technique for the manufacturing of the fiber network. However, current electrospinning processes are too slow and expensive to be viable for a commercial application. In order to bring the technology closer to industry, it would be desirable to be able to simplify the fiber fabrication, or outright use existing commercial alternatives.

This chapter described the experimental research work done on SMFCs within the scope of this thesis. Instead of using electrospun nanofibers, commercially available non-woven fiber networks have been explored in order enable mass production and potentially commercially viable materials. Two different fibers have been investigated: Silver plated nylon fibers (Paper C) and carbon fiber (Paper B).

Pressure assisted infiltration of molten solder

Regardless of fiber and alloy composition, the principle for forming the composite structure is the same. It is based upon pressure assisted infiltration of solder in the molten state into the fiber network. The difficulty of infiltration depends on the wetting between the solder and fiber. Molten metal has a relatively large surface tension , and has poor wetting towards most polymers. Therefore, surface modifications such as metal coatings and high pressure during infiltration can be needed on order to ensure proper infiltration of the matrix [97, 166].

For the infiltration process, custom in-house constructed tools were used. The fiber network was placed inside a thin mold cavity, which was heated to 30°C above the melting point of the metal. Molten metal from a separate melt cavity is then injected under pressure into the mold, and the pressure is maintained for several seconds. The end result is a thin preform foil of the composite material, which can be cut into arbitrary shapes in order to fit desired application.

Two different versions of the infiltration tool were used. The first is a lab scale prototype which has been used in previous works in our group, which can produce single round pieces with a diameter of 30 mm. The second is a newly developed automated machine, for volume production on a roll-to-roll basis. This machine can produce 100x100 mm pieces at a rate of tens per hour.

Thermal characterization

To evaluate the performance of the fabricated SMFCs in a TIM application, the fabricated SMFCs were sandwiched between Electroless Nickel Immersion Gold (ENIG) coated Cu surfaces. A pressure of 200 kPa was applied to the stack, and fluxless reflow was carried out using a temperature profile optimized depending on solder material used. After reflow, the resulting three-layer sandwich structure was used to characterize the thermal properties of the TIM.

The main tool for thermal characterization used in this thesis was the transient laser flash method. The principle is based on heating one side of a specimen with a laser pulse and monitoring the time-dependent temperature change on the opposite side using an IR detector. Under perfect adiabatic conditions, the temperature response from the laser pulse depends on the thickness d and thermal diffusivity α of the specimen according to:

$$\alpha = \frac{1.38d^2}{\pi^2 t_{1/2}} \tag{3.1}$$

where $t_{1/2}$ is the half rise time of the temperature. With additional corrections, it is possible to extract the thermal diffusivity even under non-adiabatic conditions. The thermal diffusivity is further related to the thermal conductivity λ according to:

$$\lambda = \rho C_p \alpha \tag{3.2}$$

where ρ is the density and C_p is the specific heat capacity of the specimen.

From this we can calculate its effective thermal conductivity. In a multilayer setup, it is possible to extract the thermal resistance contribution of a single layer given that the the properties of the other layers is known. In a three-layer model, with a TIM between two substrates, the thermal interface resistance R_{TIM} relates to the measured $\lambda_{effective}$ by the following equation:

$$\frac{d_{total}}{\lambda_{effective}} = \frac{d_{s1}}{\lambda_{s1}} + \frac{d_{s2}}{\lambda_{s2}} + R_{TIM} \tag{3.3}$$

where d_{s1}, d_{s2} are the thickness and λ_{s1}, λ_{s2} the thermal conductivity of the two substrates. In practice, this is best done using more complex numerical analysis software, but the equation above serves to demonstrate the principle.

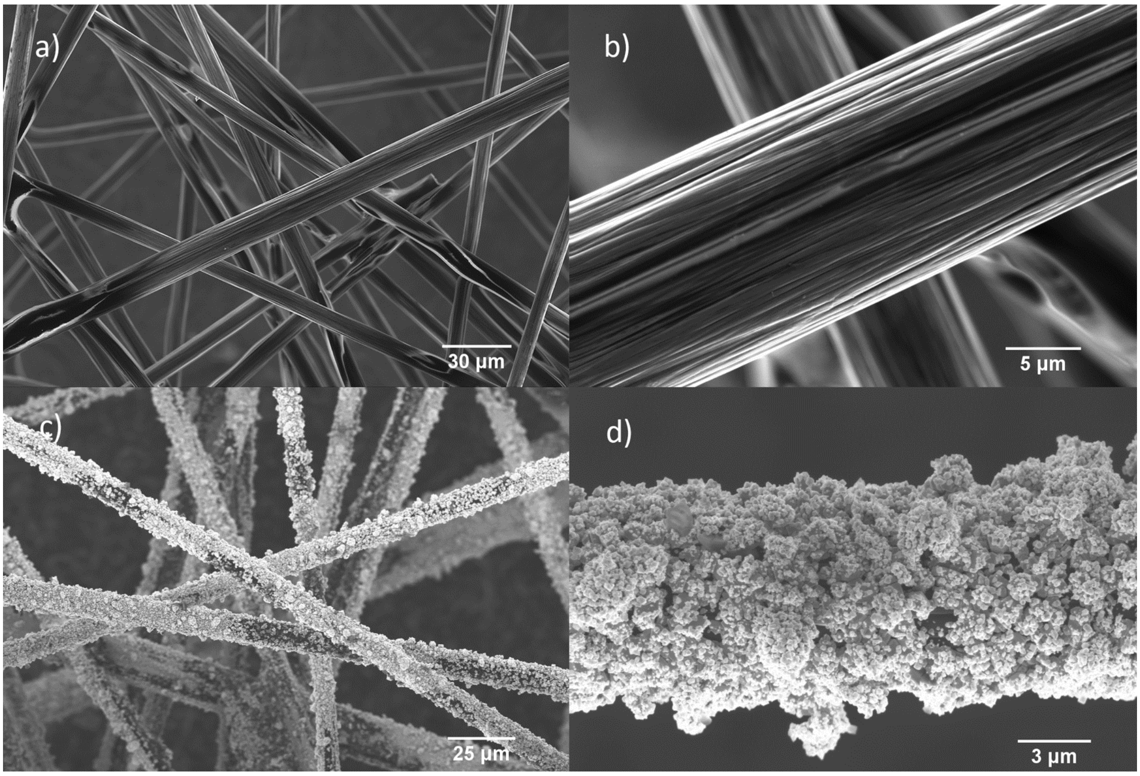

Figure 3.2: SEM images of carbon fiber network, pristine (a,b) and with a Ag plating layer (c,d)

3.2 Carbon Fiber Composite

Carbon fiber (CF) is widely used as a component in high performing composite materials, primarily owing to its high strength. In addition, like other carbon allotropes, CFs have high thermal conductivity, which could be increase the thermal performance of a CF composite [167]. Murugesan et al. demonstrated a SMFC with SAC solder matrix and electrospun CFs from mesophase pitch [98]. However, as previously explained, it would be desirable to be able utilize fibers that are available at a commercially relevant scale.

In paper B we instead use a procured non-woven CF veil, which is available in large quantities on rolls. SEM images of the fiber network can be seen in figure 3.2 a and b. The fiber networks consists of CF with a diameter of 8 ± 2 μ m and the total mat thickness is 82 ± 3 μm, with a total fiber volume fraction of around 4 %.

This fiber size is around one order of magnitude larger than that of the fibers produced by electrospinning, and the pore size between fibers is similarly larger. For the electrospun CF network, a metal coating to facilitate wetting between fiber and matrix was required in order to properly manage inflitration, despite the fact that the wetting between solder and graphite is relatively good [168]. However, with a more sparse matrix, this metal coating might not be required. Thus, the infiltration was attempted both with pristine fiber networks and with Ag coated fibers. The Ag coating was formed by a chemical method. A silver nitrate solution was saturated with ammonia to form diamine silver complex, which in turn was mixed with a

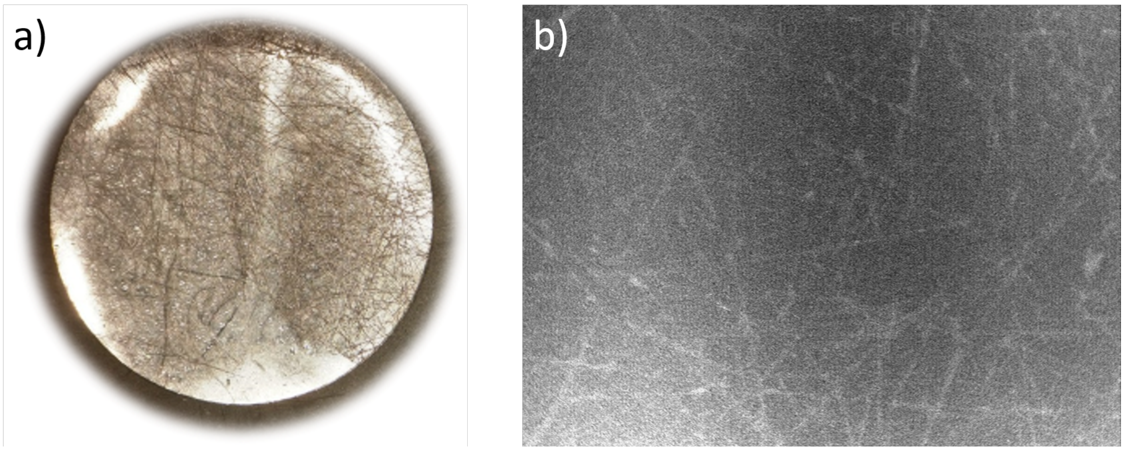

Figure 3.3: a) Photo of the infiltrated CF-SMFC preform. b) X-ray image of the assmebled TIM sandwich structure.

mixture of glucose and tataric acid to form deposit silver on the fiber network. The silver plated fiber can be seen in figure 3.2c and d.

Despite the fact that the CF fiber is available as a roll, the manual prototype infiltration equipment was used for the fabrication of the CF-SMFC in this work, due to a process incompatibility. The problem is not insurmountable, and future works aims to adapt the process in order to create high volume TIM. SAC305 (96.5%Sn-3%Ag-0.5%Cu) alloy was used as matrix material, as it is one of the most common solders used in industry today.

The resulting preform TIM after infiltration can be seen in figure 3.3 a. After subsequent reflow the internal structure of the TIM without Ag plating was characterized using X-ray imaging, the result of which can be seen in figure 3.3 b. The x-ray image provides contrast based on difference in density, and is useful to detect voids and imperfect infiltration. As seen from the image, the density is uniform throughout the sample, with only the outline of the fibers themselves providing any contrast. This indicates that the wetting between the fibers and the matrix is good despite the lack of metallization on the fiber surface. This is further confirmed by later thermal characterization, and so only the pristine CF TIM was further investigated.

3.3 Nylon Fiber Network Composites

Among the different fiber compositions investigated for SMFCs in the past, the majority have used polymer fibers, mainly polyimide (PI) [163–165]. The reason for this is that polymers are soft materials which may help decrease the modulus of the TIM and reduce thermal stresses. Similarly to the case with CF, a commercially available fiber alternative would be desirable, and in paper C we investigate new version of SMFC based on commercially available polymer fibers.

Instead of PI fibers, these commercial fibers consists of polyamide (PA), or nylon, more specifically PA6,6. It is one of the most common type of nylon in the plastics and textile industries, making it cheap and abundant. The fiber procured (Statex,

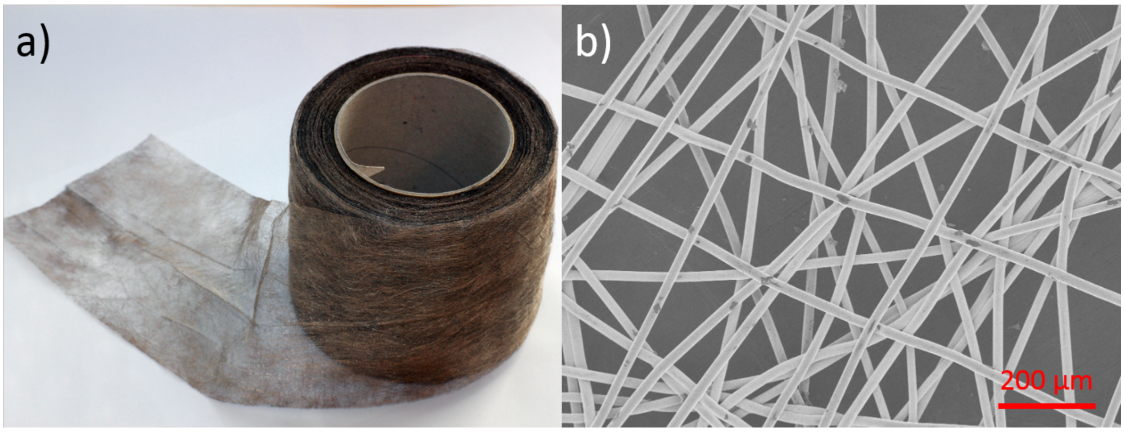

Figure 3.4: A roll of the commercial Ag-plated PA6,6 fiber network.

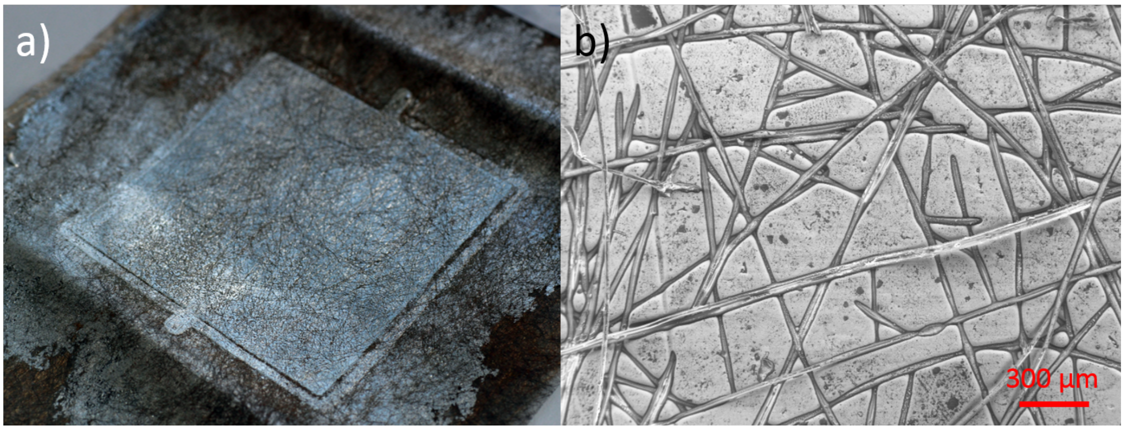

Figure 3.5: a) Resulting TIM on the fiber roll. b) SEM image of fabricated TIM surface.

Bern) is a non-woven PA6,6 fabric with a Ag coating. The Ag coating is necessary since PA6,6 has very poor wetting towards solders unlike CF. Since the fabric is already coated, no additional treatment of the fibers is needed before infiltration. The fiber is available on rolls, as can be seen in figure 3.4 a. The microstructure of the fiber network can be seen in figure 3.4 b. The fiber network consists of randomly aligned fibers with a fiber diameter of 8 μm, which forms a mat with a thickness of 80 μm at a volumetric filling factor of 4%.

In this study, a newly developed automated infiltration equipment was used. Instead of placing the fiber inside a cavity into which the molten metal is injected, the cavity is formed from two tooling halves clamping onto the fiber, forming a cavity around part of the fiber, with the fiber mat itself sealing the cavity between the tooling halves. After this, molten metal is injected under high pressure, filling up the cavity and infiltrating the fibers.

The result is a 50x50 mm square TIM sample still attached to the fiber film, which can be seen in figure 3.5 a. Note that around the TIM sample, the fiber is compresed during infiltration, and is supposed to provide a seal. However, as can be seen in the image, some metal has penetrated the fiber around the sample, which may

Table 3.1: SMFC sample configurations

Sample configuration:	Metal	No. of fiber mat layers	Thickness after infiltration (μm)	BLT after reflow (μm)
A	SAC	1	220	68 ± 3
B	SAC	2	220	90 ± 13
C	SAC	3	220	117 ± 3
D	In	1	175	44 ± 3
E	In	2	175	86 ± 13

relax the pressure somewhat. Thus, it is difficult to tell the true pressure attained during this infiltration, though the infiltration appears to be successful from visual as well as SEM inspection (figure 3.5 b).

Multiple layers of fiber mat were stacked before infiltration in order to investigate the effect of fiber concentration in the SMFC. The fiber mat layers will compress into each other during reflow, increasing the concentration of fiber compared to the matrix with increasing number of fiber mat layers. Two different matrix materials were used, SAC305 and pure indium, as these are the two most common materials for solder TIM, as well as the most studied matrices in previous reports [97, 165]. In total, five different matrix/fiber configurations were investigated, according to table 3.1

The thickness of the TIM sample depends on the cavity halves together with the thickness of the fiber network, although it is significantly compressed. By exchanging cavity the thickness can be varied, while differing number of fiber layers compress into each other enough that no discernible difference could be found on the final thickness. Regardless, during the reflow process, excess material was pressed out of the interface, thinning the composite until the fiber phase supports the applied pressure, leading to a reduced BLT compared to the initial thickness.

To compare the SMFC to regular solder, reference samples with pure SAC and indium at the interface were prepared from solder preforms (Indalloy #4 and #256, Indium Co.) using an identical reflow profile. However, without the fiber component, the applied pressure will squeeze out almost all material from the interface, creating a very thin bond line. In order to make a comparison, copper spacers were created to ensure a similar BLT as for the SMFC TIM.

An X-ray microscope was used in order to investigate the internal structure of The assembled TIM structures. Figure 3.6 a-b, d-e and g-h show the assembled structure for sample condition A, B and C respectively. Light parts indicate regions of lower density, while the dark regions show continuous metallic thermal paths between the joined surfaces. The contrasting features consist of the fiber network together with intermittent small voids throughout the material. While voids inside a solder joint can affect the thermal and mechanical performance negatively[169, 170], it is mainly through large voids, which can lead to hot spots and delamination. Small, evenly spread voids do not necessarily contribute to decreased reliability at moderate void levels[171], and could even potentially be beneficial through stress

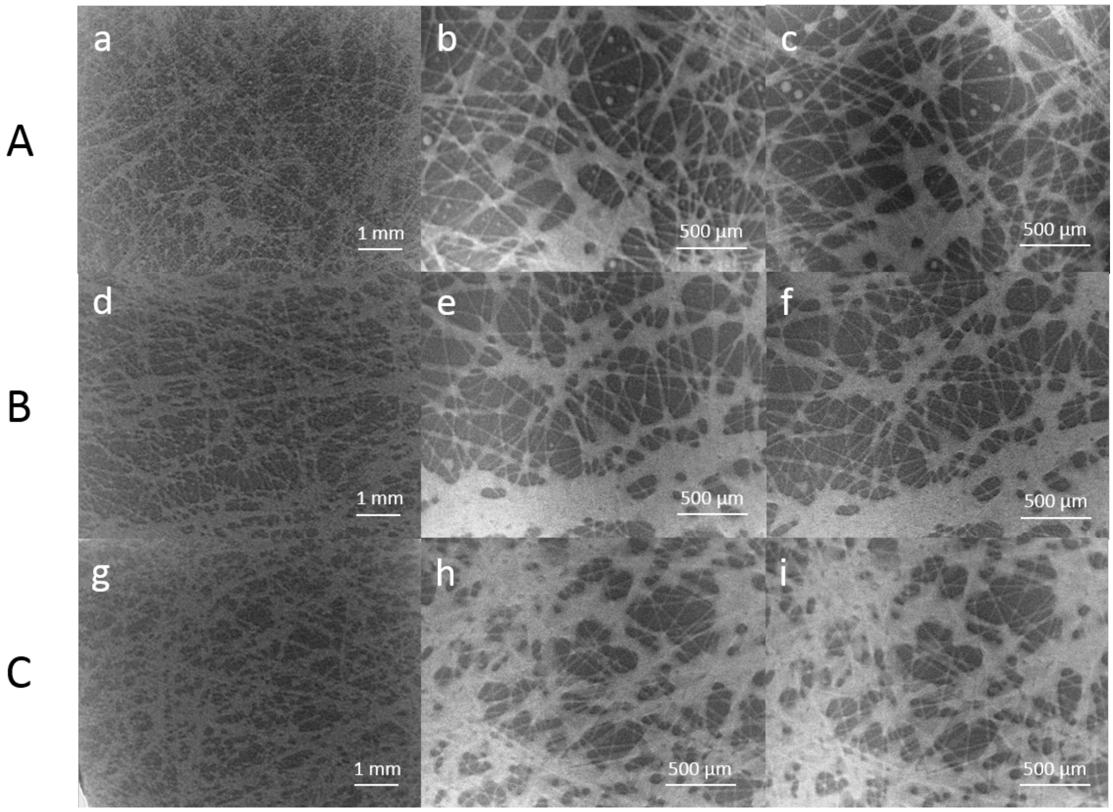

Figure 3.6: X-ray images of the composite material in a TIM assembly, after reflow, for one (a,b), two (d,e) and three (g,h) fiber network layers (sample condition A, B and C respectively) Same samples after thermal cycling (c,f,i).

relaxation and as crack propagation barriers. In this case the voids are evenly spread out at the millimeter scale, although the amount of voids starts to raise concerns at three fiber network layers. However, how much this affects the thermal properties can be measured directly by thermal interface resistance measurements.

Tensile analysis

One of the main motivations for the polymer composite is to modify the mechanical properties of the TIM compared to pure solder. To investigate this phenomenom, the samples were subjected to a pulling test in order to measure Young's modulus and tensile behavior of the different configurations. The SMFC was cut into strips of 10 x 50 mm, clamped at each edge and pulled with a strain rate of 0.1 mm/minute for indium based samples and 0.3 mm/minute for SAC based samples, with metallic foils of pure indium and SAC as references.

Figures 3.7 a and b show the stress-strain curves for SAC based and Indium based composites respectively. Figure 3.7 c shows all test conditions in the linear regime at low strain, from which the Young's modulus can be calculated. The values for the Young's modulus are presented in table 3.2.

The values of the reference SAC and indium foils significantly differ from the bulk literature values (Indium: 88 W/mK[172], SAC: 60 W/mK[10]) of the alloys.

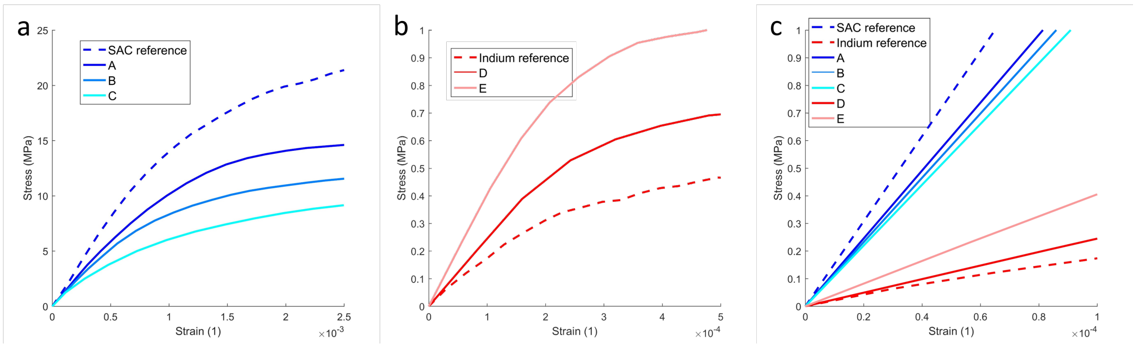

Figure 3.7: Tensile behavior of a) SAC based SMFCs with pure SAC reference, b) Indium based SMFCs with pure indium reference. c) Initial linear regime tensile slope for all samples with pure solder references.

However, the tested material has been exposed to processing with high temperatures and pressure, which may significantly alter the mechanical properties[173, 174]. In addition, size effects due to the low thickness can have a large effect on the properties of thin metallic foils[175]. The lower Young's modulus measured in this work is consistent with earlier reports of tensile measurements on thin metallic foils[176–178]. Thus, while the values reported here should not be taken at face value, they can still be useful for comparative purposes.

For the SAC based composite, a clear trend of decreased stiffness with increased fiber content can be seen (figure 3.7 a). A contribution both from the low Young's modulus of the fibers as well as an increase in voids trapped inside the material can be expected to contribute to this decrease. This depression in stiffness is consistent with a similar report by Zandén et al. [97], in which a SMFC based on SAC and electrospun polyimide was investigated.

Indium based SMFCs on the other hand, show an inverse trend, with increased elastic modulus and increased strength with additional fiber network layers (figure 3.7 b). This behavior is more difficult to explain, as the individual components in the composite all have a lower modulus. But again, this is consistent with a previous work, where Luo et al. investigated the tensile behavior of a SMFC based on Indium and electrospun polyimide fiber[162]. Luo et al. found a mutual strengthening mechanism between the fiber and matrix, which increased the total strength of the composite. The tensile behaviour of the SMFC in this work indicates that the same mechanism plays a role in this case as well, despite a large difference in average fiber diameter (780 nm vs 8 μm in this work).

Figure 3.7 c shows the linear regime of all sample configurations. By varying the matrix material and fiber density, the elastic modulus can be tailored in the regime between the two pure materials. Further optimisation would allow for the engineering of composite materials with very specific mechanical properties.

Note that the tensile testing is done directly on the SMFC prior to assembly and reflow in an application. Since a significant amount of metal is ejected from the interface during reflow, the actual fiber density of the TIM in application will be higher. Thus, the changes in mechanical properties can be expected to be even more pronounced, although to what degree is to be further investigated in future works.

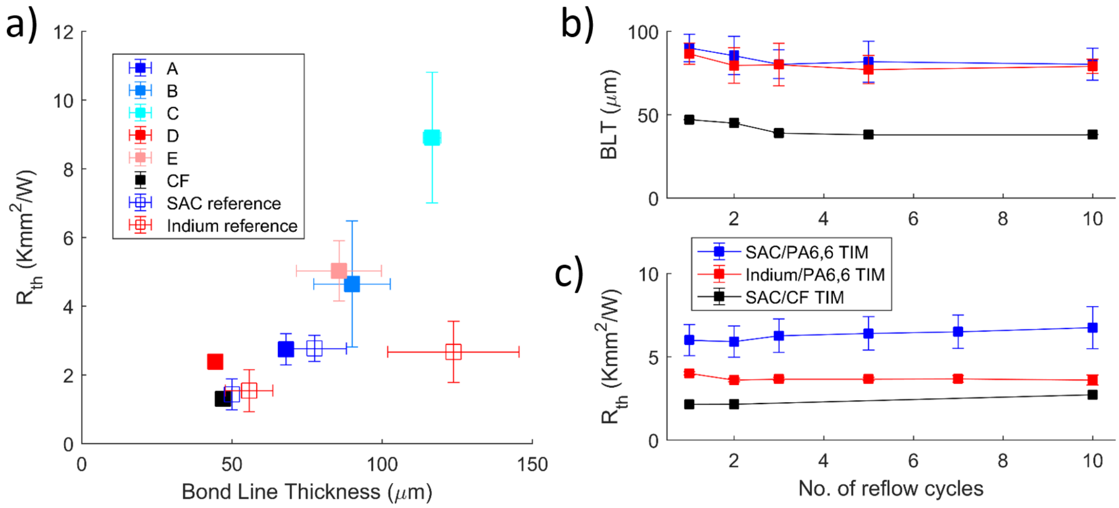

Figure 3.8: a) Thermal interface resistance versus BLT for all test conditions (Filled squares) and pure solder references (unfilled squares). b) BLT as a function of number of reflow cycles for test condition B (blue), E (red) and CF (black). c) Thermal interface resistance as a function of number of reflow cycles for test condition B (blue), E (red) and CF (black).

3.4 Thermal Results

As the most important figure of merit, the thermal interface resistance was measured for all configurations, both with CF and PA6,6 fibers. The results are shown in figure 3.8 a, plotted versus the BLT. As expected, increasing the amount of fiber network layers increases the BLT and the thermal interface resistance. However, the difference in thermal interface resistance with respect to variation of the number of layers is larger than for a material with uniform thermal conductivity. With increasing amount of fiber network layers, the layers compress into each other and the total fiber network density increases. Increasing fiber density leads to a decreased thermal conductivity due to the drastically lower thermal conductivity of PA6,6 (0.25 W/mK) compared to SAC alloy (60 W/mK) and Indium (82 W/mK). The increased fiber density also reduces the infiltration effectiveness and traps additional voids in the interface, further reducing the effective composite thermal conductivity.

SAC based and Indium based samples have a similar thermal interface resistance compared to number of fiber mat layers. A lower thermal interface resistance of samples based on Indium could be expected considering the increased thermal conductivity of Indium compared to SAC, and the absence of such difference indicates that the bulk thermal conductivity of the solder material is not the limiting factor for the total thermal interface resistance, and that SAC is possibly slightly more compatible with the infiltration process. It should be noted however, that the higher effective thermal conductivity of configuration A as compared to configuration D can be explained by a higher fiber density due to the same amount of fibers inside a thinner interface. The total thermal interface resistance is instead primarily based on the number of fiber layers rather than the BLT.

Using a single fiber mat layer, the thermal interface resistance of the composite is

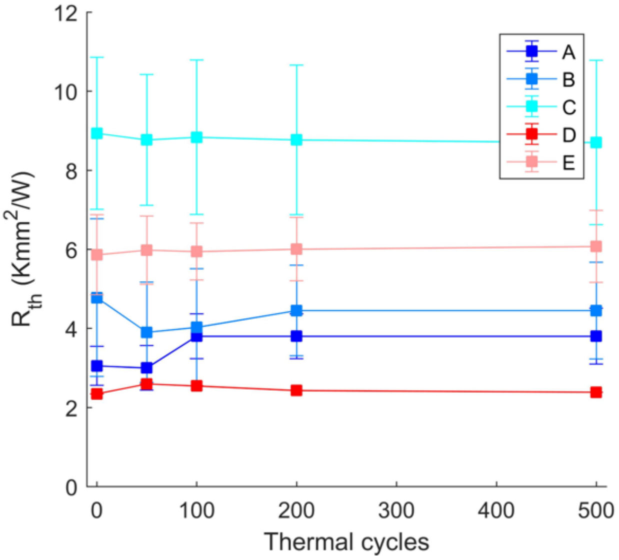

Figure 3.9: Thermal interface resistance as a function of number of cycles during temperature cycling for PA6,6 based SMFCs.

still close to the reference samples with pure solder, which indicates that any extra voids due to the presence of the fiber network is limited for single-layer fiber networks. However, we can see the superior wetting characteristics of SAC/CF compared with the other configurations, as the thermal resistance here is almost identical with the SAC reference sample. This indicates that the presence of fibers in the CF TIM does not harm the thermal performance in any way.

While the thermal interface resistance of the SMFC is comparable to pure solders, a potential benefit of the composite compared to conventional solders is the possibility of a fluxless reflow process without using complicated spacers or frames to prevent metal pump-out of the interface. The fiber network in the composite acts as a spacer, ensuring a well-defined and uniform BLT throughout the sample. To confirm that a consistent BLT is achievable over several reflow cycles, samples from configuration B, D, and CF were subjected to additional reflow cycles while monitoring BLT and thermal interface resistance.

Figure 3.8 shows the BLT (3.8b) and thermal interface resistance (3.8c) across 10 reflow cycles. A slight decrease in BLT and increase in thermal interface resistance is seen at first, attributed to a slight additional compression of the fibers, but the performance subsequently remains stable. Note that the interface does compress during the initial reflow until the fiber network is compressed enough to withstand the applied pressure. However, subsequent additional melting of the interface does not cause additional material to escape.

A comparable reflow cycle with pure solder without the use of a spacer immediately collapses the interface (BLT <10 μm) and the melt leaks out of the interface. To be able to apply the composite in an application as a preform with built-in BLT control could potentially eliminate the need for spacer usage, and allow for significantly simplified process flow for TIM assembly.

Table 3.2: Thermal and mechanical results for SMFC configurations

Sample configuration	BLT (μm)	λ_{eff} (W/mK)	R_{TIM} (Kmm^2/W)	Young's modulus (GPa)
A	68 ± 3	25 ± 4	2.7 ± 0.5	11.6
B	90 ± 13	19 ± 5	4.6 ± 1.8	9.5
C	117 ± 3	13 ± 2	8.9 ± 1.9	7.8
D	44 ± 3	18 ± 1	2.4 ± 0.1	3.0
E	86 ± 13	17 ± 2	5.0 ± 0.9	3.8
CF	47 ± 1	35 ± 2	1.4 ± 0.4	
SAC references	50 ± 1	34 ± 1	1.4 ± 0.5	18.0
	78 ± 10	28 ± 4	2.8 ± 0.4	
Indium references	56 ± 8	36 ± 5	1.5 ± 0.6	1.9
	123 ± 22	46 ± 8	2.7 ± 0.9	

Additionally, the reliability of the PA6,6 based SMFCs was tested using thermal cycling in accordance with JEDEC standard test condition 1. The samples were subjected to 500 cycles, with a temperature profile ranging from -40°C to 115°, at 2 cycles/h and 5 min soak time at each extreme. Thermal interface resistance measurements were carried out periodically to monitor the change in thermal interface resistance. Figure 3.9 shows measured thermal interface resistance values during thermal cycling. Each test case is an average of at least 3 samples. All samples across showed a variation of less than 20% over the full amount of cycles, indicating that internal structure of the TIM does not change significantly due to thermal stress. This is seen clearly in figure 3.6, where images of the same spot before (b, e, h) and after (c, f, i) 500 thermal cycles show the same distribution of fibers and voids. The X-ray images show an absence of even minor structural changes which could be indicative of reliability issues further along.

3.5 Summary and Conclusion

The thermal and mechanical characterizations of the different versions of SMFCs are summarized in table 3.2. Figure 3.10 further shows the thermal performance versus BLT of the different SMFCs compared to a selection of previously reported metal based TIM (blue) and commercial thermal greases (pink) from the earlier review in chapter 2. The dashed lines indicates hypothetical TIMs with thermal conductivity as indicated and a thermal contact resistance of 1 Kmm^2/W as comparison. SMFCs from earlier works typically fall in the range between the hypothetical 20 W/mK and 40 W/mK TIMs. Pure metals or alloys, such as Gallium[80, 81], In-Bi-Sn[81], Sn-Bi[79] and sintered silver nanoparticles[84] are typically slightly higher, although by achieving very thin bond lines it is still possible to achieve a low thermal interface resistance. Composite stuctures such as the solder-graphite network reported by Sharma et al.[95] follow the same trend, and the only outlier is a liquid phase sintered Cu-In composite[87] which takes advantage of the much higher thermal conductivity

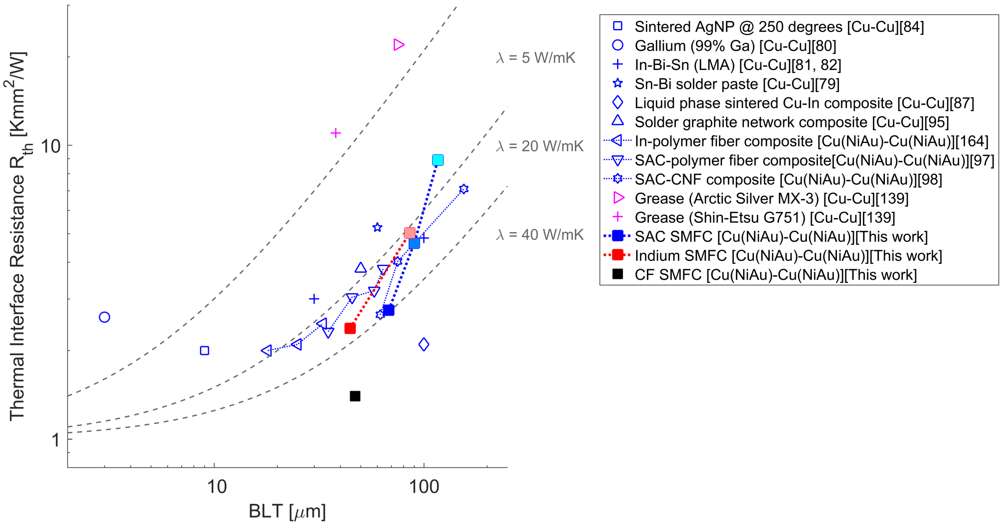

Figure 3.10: Comparison of thermal interface resistance versus BLT for various metal based TIM (blue), commercial thermal grease (pink) and this work (blue, red and black filled squares).

of Cu.

Most metal based TIMs still have a similar thermal performance as pure solder, and this will not change without the addition of other materials with significantly higher intrinsic thermal conductivity, such as carbon based materials[109] or non-solderable metals[87, 179]. However, despite little further improvement in thermal interface resistance, solder based TIMs can still be improved with regards to mechanical properties and handling characteristics. The TIMs in this work fall in the same range for one and two-layer samples, indicating that the these SMFCs can act as replacement for solder. For the CF based TIM, it is even lower than previously reported metal TIM.

In conclusion, with the CF TIM, we have shown that it's possible to make SMFCs with very low thermal resistance using commercially available fibers. However, CFs have very high stiffness, and might not improve the mechanical properties of the TIM significantly, although the benefits in BLT control and handling is still present. For the PA6,6 based TIM, we have shown how the mechanical properties of the TIM can be modified based on different material selections and compositions, while retaining good thermal properties. This allows us to tailor the TIM towards specific applications where current materials are unsatisfactory.

Chapter 4

Conclusion and outlook

This thesis contributes to the field of thermal interface materials research through a thorough review of the field as well as experimental work on solder matrix fiber composite TIMs.

The first part of the thesis investigates the different trends within novel TIM research. Three main categories are identified, and each treated in terms of novel research, trends and potential for future research. First, particle laden polymers have, despite investigations into high thermal conductivity fillers such as graphene and carbon nanotubes, not been able to improve the performance of novel compounds over that of already existing commercial compounds. Second, continuous phase metal TIM have excellent thermal conductivity, but reliability is a concern, and most research is focused on modifying the mechanical properties while retaining low thermal interface resistance. Third, CNT array TIM show great promise as future TIM with thermal performance in the range of solders, together with complete thermomechanical decoupling. However, the reliability has not yet been confirmed, and methods for producing CNTs in a large scale is required before widespread application is possible.

Finally, several novel types of TIM are presented, including thermally conductive polymers, mechanically deformed metal and novel carbon based TIM. Together they give an overview of the field and could be a useful tool to gain an overview of the field for new researchers or researchers from other fields.

The second part of the thesis describes experimental work on solder matrix fiber composite TIM. The concept has already been investigated by researchers from out lab, but previous research was reliant on complicated and expensive processing. In this thesis, we investigate SMFCs using two different commercially available fibers: carbon fibers and Ag coated nylon fibers. The fibers were investigated as composites together with In and SAC solder matrices.

The studies show how the fiber phase modify the thermal, mechanical and handling properties of the original solder. By varying the concentration of fibers in the TIM, the properties of the composite can be tailored towards specific applications, potentially opening up new applications which place particular demands on the TIM. At moderate fiber concentrations, the thermal interface resistance was similar to pure solder TIM, indicating that the fiber presence does not significantly affect the thermal performance. The SMFC presented in this work represents a step on the path from research to industrial applications.

Acknowledgments

This thesis is would not have been possible without the help and support from the people around me. I would like to thank my supervisor and examiner Johan Liu for giving me the opportunity to work in an exciting field in an unrestrained manner. I would also like to express my gratitude to my co-supervisors, Lilei Ye and Torbjörn Nilsson, for their guidance and support whenever I needed it. I am also grateful for their work in helping me write my papers and this thesis, without which the end results would have suffered greatly.

I would like to thank all my colleagues and coworkers in the EMSL packaging group I have had during my time working here, among others: Hafid Zehri, Majid Kabiri Samani, Yifeng Fu, Nan Wang, Ning Wang, Yong Zhang, Wei Mu, Di Jiang, Michael Edwards, Si Chen, Nikolaos Logothetis, Peng Su and Marti Gutierrez Latorre. Thank you for all your friendship, help and for a great working environment. A special thanks to Andreas Nylander, for constant help and daily discussions in matters large and small.

I would also like to thank my family and friends, for love and support, for keeping me grounded in reality and for showing me what it really important. Finally, Jennifer Panditha, whose love and unwavering support has been a guiding beacon for so long, and without whom I would never have come this far.

This work was supported by the Swedish Foundation for Strategic Research (SSF) under contract (Nos SE13-0061, GMT14-0045), the Production Area of Advance at Chalmers University of Technology and EU Horizon 2020 project “Smartherm”.

Josef Hansson
Göteborg, April 2018

Bibliography

[1] Khosrow Ebrahimi, Gerard F Jones, and Amy S Fleischer. “A review of data center cooling technology , operating conditions and the corresponding low-grade waste heat recovery opportunities”. In: *Renewable and Sustainable Energy Reviews* 31 (2014), pp. 622–638. ISSN: 1364-0321. DOI: `10.1016/j.rser.2013.12.007` (cit. on p. 1).

[2] ITRS. “International Technology Roadmap for Semiconductors - Emerging Research Materials Summary”. In: (2013) (cit. on p. 2).

[3] Gerald L Pollack. “Kapitza Resistance”. In: *Reviews of Modern Physics* 41-81.1 (1969), p. 48. DOI: `10.1103/RevModPhys.41.48` (cit. on p. 6).

[4] Sreekant Narumanchi, Mark Mihalic, Kenneth Kelly, and Gary Eesley. “Thermal interface materials for power electronics applications”. In: *2008 11th Intersociety Conference on Thermal and Thermomechanical Phenomena in Electronic Systems* (2008), pp. 395–404. ISSN: 1087-9870. DOI: `10.1109/ITHERM.2008.4544297` (cit. on p. 8).

[5] Ram Viswanath, Manufacturing Group, and Intel Corp. “Thermal Performance Challenges from Silicon to Systems”. In: *Intel Technology Journal Q3,* (2000), pp. 1–16 (cit. on pp. 8, 9).

[6] Daniel Blazej. *Thermal Interface Materials.* 2003. URL: `http://www.electronics-cooling.com/2003/11/thermal-interface-materials/` (visited on 02/26/2016) (cit. on pp. 8, 9).

[7] Xingcun Colin Tong. *Advanced Materials for Thermal Management of Electronic Packaging.* Vol. 30. Springer, 2011, p. 347. ISBN: 978-1-4419-7758-8. DOI: `10.1007/978-1-4419-7759-5` (cit. on p. 8).

[8] L Maguire, M Behnia, and G Morrison. “Systematic evaluation of thermal interface materials—a case study in high power amplifier design”. In: *Microelectronics and Reliability* 45.3-4 (2005), pp. 711–725. ISSN: 00262714. DOI: `10.1016/j.microrel.2004.10.030` (cit. on p. 8).

[9] Mathias Ekpu, Raj Bhatti, Ndy Ekere, Sabuj Mallik, and Kenny Otiaba. “Effects of Thermal Interface Materials (Solders) on Thermal Performance of a Microelectronic Package”. In: *Dtip* April (2012) (cit. on p. 8).

[10] Jum Wilson. *Thermal Conductivity of Solders.* 2006. URL: `http://www.electronics-cooling.com/2006/08/thermal-conductivity-of-solders/` (visited on 03/03/2016) (cit. on pp. 8, 32).

[11] John A Emerson, Michael J Rightley, Jeffrey A Galloway, David F Rae, Dale L Huber, and Eric J Cotts. "Minimizing the Bondline Thermal Resistance in Thermal Interface". In: *Physics* (2005), pp. 106–111 (cit. on p. 8).

[12] Ravi S. Prasher and James Chris Matayabas. "Thermal contact resistance of cured gel polymeric thermal interface material". In: *IEEE Transactions on Components and Packaging Technologies* 27.4 (2004), pp. 702–709. ISSN: 15213331. DOI: `10.1109/TCAPT.2004.838883` (cit. on p. 8).

[13] *Gap Pad Products*. 2016. URL: `http://www.bergquistcompany.com/thermal%7B%5C_%7Dmaterials/gap-pad.htm` (visited on 03/03/2016) (cit. on p. 8).

[14] Miksa de Sorgo. *Understanding Phase Change Materials*. 2002. URL: `http://www.electronics-cooling.com/2002/05/understanding-phase-change-materials/` (visited on 03/03/2016) (cit. on p. 8).

[15] *Thermally Conductive Adhesives*. 2016. URL: `http://www.epoxies.com/products/thermally-conductive/` (visited on 03/03/2016) (cit. on p. 8).

[16] G Bischak and C Vogdes. "Thermal management design criteria and solutions". In: *Wescon/98. Conference Proceedings (Cat. No.98CH36265)*. IEEE, 1998, pp. 188–193. ISBN: 0-7803-5078-2. DOI: `10.1109/WESCON.1998.716447` (cit. on p. 8).

[17] R. Prasher. "Thermal Interface Materials: Historical Perspective, Status, and Future Directions". In: *Proceedings of the IEEE* 94.8 (2006), pp. 1571–1586. ISSN: 0018-9219. DOI: `10.1109/JPROC.2006.879796` (cit. on p. 9).

[18] Hatsuo Ishida and Sarawut Rimdusit. "Very high thermal conductivity obtained by boron nitride-filled polybenzoxazine". In: *Thermochimica Acta* 320.1-2 (1998), pp. 177–186. ISSN: 00406031. DOI: `10.1016/S0040-6031(98)00463-8` (cit. on p. 10).

[19] Wen-Ying Zhou, Shu-Hua Qi, Hong-Zhen Zhao, and Nai-Liang Liu. "Thermally Conductive Silicone Rubber Reinforced With Boron Nitride Particle". In: *Polymers and Polymer Composites* 28.2 (2007), pp. 23–28. ISSN: 09673911. DOI: `10.1002/pc.20296` (cit. on p. 11).

[20] Kisang Ahn, Kiho Kim, and Jooheon Kim. "Fabrication of surface-treated BN/ETDS composites for enhanced thermal and mechanical properties". In: *Ceramics International* 41.8 (2015), pp. 9488–9495. ISSN: 02728842. DOI: `10.1016/j.ceramint.2015.04.006` (cit. on p. 11).

[21] Zifeng Wang, Yuqiao Fu, Wenjun Meng, and Chunyi Zhi. "Solvent-free fabrication of thermally conductive insulating epoxy composites with boron nitride nanoplatelets as fillers." In: *Nanoscale research letters* 9.1 (2014), p. 643. ISSN: 1931-7573. DOI: `10.1186/1556-276X-9-643` (cit. on p. 11).

[22] Ziyin Lin, Yan Liu, Sathyanarayanan Raghavan, Kyoung Sik Moon, Suresh K. Sitaraman, and Ching Ping Wong. “Magnetic alignment of hexagonal boron nitride platelets in polymer matrix: Toward high performance anisotropic polymer composites for electronic encapsulation”. In: *ACS Applied Materials and Interfaces* 5.15 (2013), pp. 7633–7640. ISSN: 19448244. DOI: `10.1021/am401939z` (cit. on pp. 11, 22).

[23] Yeon Kyung Shin, Woo Sung Lee, Myong Jae Yoo, and Eung Soo Kim. “Effect of BN filler on thermal properties of HDPE matrix composites”. In: *Ceramics International* 39.SUPPL.1 (2013), S569–S573. ISSN: 02728842. DOI: `10.1016/j.ceramint.2012.10.137` (cit. on pp. 11, 12).

[24] Zhengkai Yuan, Jinhong Yu, Zihai He, Xinfeng Wu, Baolin Rao, Shaorong Lu, and Nan Jiang. “Improved thermal properties of epoxy composites filled with thermotropic liquid crystalline epoxy grafted aluminum nitride”. In: *Fibers and Polymers* 15.12 (2014), pp. 2581–2590. ISSN: 1229-9197. DOI: `10.1007/s12221-014-2581-x` (cit. on p. 11).

[25] Hui Yu, Liangliang Li, Teruo Kido, Guannan Xi, Guangchen Xu, and Fu Guo. “Thermal and insulating properties of epoxy/aluminum nitride composites used for thermal interface material”. In: *Journal of Applied Polymer Science* (2011), pp. 1763–1772. ISSN: 09673911. DOI: `10.1002/app.35016` (cit. on p. 11).

[26] K S Novoselov, A K Geim, S V Morozov, D Jiang, Y Zhang, S V Dubonos, I V Grigorieva, and A A Firsov. “Electric field effect in atomically thin carbon films.” In: *Science* 306.5696 (2004), pp. 666–669. ISSN: 1095-9203. DOI: `10.1126/science.1102896`. arXiv: `0410550 [cond-mat]` (cit. on p. 11).

[27] Eric Pop, David Mann, Qian Wang, Kenneth Goodson, and Hongjie Dai. “Thermal Conductance of an Individual Single-Wall Carbon Nanotube above Room Temperature”. In: *Nano Letters* 6.1 (2006), pp. 96–100 (cit. on pp. 11, 17).

[28] P. Kim, L. Shi, A. Majumdar, and P. L. McEuen. “Thermal Transport Measurements of Individual Multiwalled Nanotubes”. In: *Physical Review Letters* 87.21 (2001), p. 215502. ISSN: 0031-9007. DOI: `10.1103/PhysRevLett.87.215502` (cit. on pp. 11, 17).

[29] M J Biercuk, M C Llaguno, M Radosavljevic, J K Hyun, A T Johnson, and J E Fischer. “Carbon nanotube composites for thermal management”. In: *Appl. Phys. Lett.* 80.15 (2002), pp. 2767–2769. ISSN: 00036951. DOI: `10.1063/1.1469696`. arXiv: `0205418 [cond-mat]` (cit. on p. 11).

[30] By Michael Bozlar, Delong He, Jinbo Bai, Yann Chalopin, Natalio Mingo, and Sebastian Volz. “Carbon Nanotube Microarchitectures for Enhanced Thermal Conduction at Ultralow Mass Fraction in Polymer Composites”. In: *Advanced Materials* (2010), pp. 1654–1658. DOI: `10.1002/adma.200901955` (cit. on p. 11).

[31] M. B. Bryning, D. E. Milkie, M. F. Islam, J. M. Kikkawa, and a. G. Yodh. “Thermal conductivity and interfacial resistance in single-wall carbon nanotube epoxy composites”. In: *Applied Physics Letters* 87.16 (2005), pp. 1–3. ISSN: 00036951. DOI: `10.1063/1.2103398` (cit. on p. 11).

[32] Scott T Huxtable et al. “Interfacial heat flow in carbon nanotube suspensions.” In: *Nature materials* 2.11 (2003), pp. 731–4. ISSN: 1476-1122. DOI: `10.1038/nmat996` (cit. on p. 11).

[33] Sergei Shenogin, Liping Xue, Rahmi Ozisik, Pawel Keblinski, and David G. Cahill. “Role of thermal boundary resistance on the heat flow in carbon-nanotube composites”. In: *Journal of Applied Physics* 95.12 (2004), pp. 8136–8144. ISSN: 00218979. DOI: `10.1063/1.1736328` (cit. on p. 11).

[34] Wei Lin, Kyoung Sik Moon, and C. P. Wong. “A combined process of in situ functionalization and microwave treatment to achieve ultrasmall thermal expansion of aligned carbon nanotube-polymer nanocomposites: Toward applications as thermal interface materials”. In: *Advanced Materials* 21.23 (2009), pp. 2421–2424. ISSN: 09359648. DOI: `10.1002/adma.200803548` (cit. on pp. 11, 20).

[35] Florian H. Gojny, Malte H G Wichmann, Bodo Fiedler, Ian A. Kinloch, Wolfgang Bauhofer, Alan H. Windle, and Karl Schulte. “Evaluation and identification of electrical and thermal conduction mechanisms in carbon nanotube/epoxy composites”. In: *Polymer* 47.6 (2006), pp. 2036–2045. ISSN: 00323861. DOI: `10.1016/j.polymer.2006.01.029` (cit. on p. 11).

[36] Zhidong Han and Alberto Fina. “Thermal conductivity of carbon nanotubes and their polymer nanocomposites: A review”. In: *Progress in Polymer Science (Oxford)* 36.7 (2011), pp. 914–944. ISSN: 00796700. DOI: `10.1016/j.progpolymsci.2010.11.004` (cit. on p. 12).

[37] Bo Tang, Guoxin Hu, Hanyang Gao, and Liuyu Hai. “Application of graphene as filler to improve thermal transport property of epoxy resin for thermal interface materials”. In: *International Journal of Heat and Mass Transfer* 85 (2015), pp. 420–429. ISSN: 00179310. DOI: `10.1016/j.ijheatmasstransfer.2015.01.141` (cit. on p. 12).

[38] Khan M F Shahil and Alexander a. Balandin. “Graphene-multilayer graphene nanocomposites as highly efficient thermal interface materials”. In: *Nano Letters* 12.2 (2012), pp. 861–867. ISSN: 15306984. DOI: `10.1021/nl203906r`. arXiv: `1201.0796v1` (cit. on pp. 12, 13).

[39] Bryan Debelak and Khalid Lafdi. “Use of exfoliated graphite filler to enhance polymer physical properties”. In: *Carbon* 45.9 (2007), pp. 1727–1734. ISSN: 00086223. DOI: `10.1016/j.carbon.2007.05.010` (cit. on p. 12).

[40] Aiping Yu, Palanisamy Ramesh, Mikhail E Itkis, Elena Bekyarova, and Robert C Haddon. “Graphite Nanoplatelet - Epoxy Composite Thermal Interface Materials”. In: *Phys. Chem C* 111.21 (2007), pp. 7565–7569 (cit. on p. 12).

[41] M. a. Raza, a. V K Westwood, a. P. Brown, and C. Stirling. “Performance of graphite nanoplatelet/silicone composites as thermal interface adhesives”. In: *Journal of Materials Science: Materials in Electronics* 23.10 (2012), pp. 1855–1863. ISSN: 09574522. DOI: `10.1007/s10854-012-0674-0` (cit. on p. 12).

[42] Wei-Li Song et al. “Polymer/carbon nanocomposites for enhanced thermal transport properties – carbon nanotubes versus graphene sheets as nanoscale fillers”. In: *Journal of Materials Chemistry* 22 (2012), p. 17133. ISSN: 0959-9428. DOI: `10.1039/c2jm32469e` (cit. on p. 12).

[43] Kafil M Razeeb and Eric Dalton. “Nanowire polymer nanocomposites as Thermal Interface Material”. In: *Advances in Nanocomposites - Synthesis, Characterization and Industrial Applications*. Ed. by Reddy Boreddy. InTech, 2011. Chap. Nanowire p, pp. 685–706. ISBN: 978-953-307-165-7. DOI: `10.5772/13959` (cit. on p. 12).

[44] Ju Xu, Alessio Munari, Eric Dalton, Alan Mathewson, and Kafil M. Razeeb. “Silver nanowire array-polymer composite as thermal interface material”. In: *Journal of Applied Physics* 106.12 (2009), p. 124310. ISSN: 00218979. DOI: `10.1063/1.3271149` (cit. on p. 12).

[45] Alessio Munari, Ju Xu, Eric Dalton, Alan Mathewson, and Kafil M. Razeeb. “Metal nanowire-polymer nanocomposite as thermal interface material”. In: *2009 59th Electronic Components and Technology Conference* (2009), pp. 448–452. DOI: `10.1109/ECTC.2009.5074052` (cit. on p. 12).

[46] Shouling Wang, Yin Cheng, Ranran Wang, Jing Sun, and Lian Gao. “Highly thermal conductive copper nanowire composites with ultralow loading: Toward applications as thermal interface materials”. In: *ACS Applied Materials and Interfaces* 6.9 (2014), pp. 6481–6486. ISSN: 19448252. DOI: `10.1021/am500009p` (cit. on p. 12).

[47] Kamyar Pashayi, Hafez Raeisi Fard, Fengyuan Lai, Sushumna Iruvanti, Joel Plawsky, and Theodorian Borca-Tasciuc. “High thermal conductivity epoxy-silver composites based on self-constructed nanostructured metallic networks”. In: *Journal of Applied Physics* 111.10 (2012), p. 104310. ISSN: 00218979. DOI: `10.1063/1.4716179` (cit. on p. 12).

[48] Kamyar Pashayi, Hafez Raeisi Fard, Fengyuan Lai, Sushumna Iruvanti, Joel Plawsky, and Theodorian Borca-Tasciuc. “Self-constructed tree-shape high thermal conductivity nanosilver networks in epoxy”. In: *Nanoscale* 6.8 (2014), p. 4292. ISSN: 2040-3364. DOI: `10.1039/c3nr06494h` (cit. on p. 12).

[49] Hyeong-Gi Lee and Kyung-Wook Paik. “Vertically aligned nickel nanowire/epoxy composite for electrical and thermal conducting material”. In: *2012 IEEE 62nd Electronic Components and Technology Conference* (2012), pp. 2087–2090. DOI: `10.1109/ECTC.2012.6249129` (cit. on p. 12).

[50] Kafil M. Razeeb and Saibal Roy. “Thermal diffusivity of nonfractal and fractal nickel nanowires”. In: *Journal of Applied Physics* 103.8 (2008), p. 084302. ISSN: 00218979. DOI: `10.1063/1.2906347` (cit. on p. 12).

[51] Nikhil Balachander, Indira Seshadri, Rutvik J. Mehta, Linda S. Schadler, Theo Borca-Tasciuc, Pawel Keblinski, and Ganpati Ramanath. "Nanowire-filled polymer composites with ultrahigh thermal conductivity". In: *Applied Physics Letters* 102.9 (2013), p. 093117. ISSN: 00036951. DOI: `10.1063/1.4793419` (cit. on p. 12).

[52] Vivek Goyal and Alexander a. Balandin. "Thermal properties of the hybrid graphene-metal nano-micro-composites: Applications in thermal interface materials". In: *Applied Physics Letters* 100.7 (2012), p. 073113. ISSN: 00036951. DOI: `10.1063/1.3687173` (cit. on p. 12).

[53] Lin Chen, Ying-Ying Sun, Jun Lin, Xiao-Ze Du, Gao-Sheng Wei, Shao-Jian He, and Sergei Nazarenko. "Modeling and analysis of synergistic effect in thermal conductivity enhancement of polymer composites with hybrid filler". In: *International Journal of Heat and Mass Transfer* 81.0 (2015), pp. 457–464. ISSN: 0017-9310. DOI: `http://dx.doi.org/10.1016/j.ijheatmasstransfer.2014.10.051` (cit. on p. 12).

[54] Geon Woong Lee, Min Park, Junkyung Kim, Jae Ik Lee, and Ho Gyu Yoon. "Enhanced thermal conductivity of polymer composites filled with hybrid filler". In: *Composites Part A: Applied Science and Manufacturing* 37.5 (2006), pp. 727–734. ISSN: 1359835X. DOI: `10.1016/j.compositesa.2005.07.006` (cit. on p. 12).

[55] Seong Yeol Pak, Hyung Min Kim, Seong Yun Kim, and Jae Ryoun Youn. "Synergistic improvement of thermal conductivity of thermoplastic composites with mixed boron nitride and multi-walled carbon nanotube fillers". In: *Carbon* 50.13 (2012), pp. 4830–4838. ISSN: 00086223. DOI: `10.1016/j.carbon.2012.06.009` (cit. on p. 12).

[56] Peng-Gang Ren, Xiao-Huan Si, Zhen-Feng Sun, Fang Ren, Lu Pei, and Si-Yu Hou. "Synergistic effect of BN and MWCNT hybrid fillers on thermal conductivity and thermal stability of ultra-high-molecular-weight polyethylene composites with a segregated structure". In: *Journal of Polymer Research* 23.2 (2016), p. 21. ISSN: 1022-9760. DOI: `10.1007/s10965-015-0908-y` (cit. on p. 12).

[57] Chih-Chun Teng, Chen-Chi M. Ma, Kuo-Chan Chiou, Tzong-Ming Lee, and Yeng-Fong Shih. "Synergetic effect of hybrid boron nitride and multi-walled carbon nanotubes on the thermal conductivity of epoxy composites". In: *Materials Chemistry and Physics* 126.3 (2011), pp. 722–728. ISSN: 02540584. DOI: `10.1016/j.matchemphys.2010.12.053` (cit. on p. 12).

[58] M.A. Raza, A.V.K. Westwood, C. Stirling, and R. Ahmad. "Effect of boron nitride addition on properties of vapour grown carbon nanofiber/rubbery epoxy composites for thermal interface applications". In: *Composites Science and Technology* 120 (2015), pp. 9–16. ISSN: 02663538. DOI: `10.1016/j.compscitech.2015.10.013` (cit. on pp. 12, 14).

[59] Yongseon Hwang, Myeongjin Kim, and Jooheon Kim. “Improvement of the mechanical properties and thermal conductivity of poly(ether-ether-ketone) with the addition of graphene oxide-carbon nanotube hybrid fillers”. In: *Composites Part A: Applied Science and Manufacturing* 55 (2013), pp. 195–202. ISSN: 1359835X. DOI: `10.1016/j.compositesa.2013.08.010` (cit. on p. 12).

[60] Hyungu Im and Jooheon Kim. “Thermal conductivity of a graphene oxide–carbon nanotube hybrid/epoxy composite”. In: *Carbon* 50.15 (2012), pp. 5429–5440. ISSN: 00086223. DOI: `10.1016/j.carbon.2012.07.029` (cit. on p. 12).

[61] Wei Yu, Huaqing Xie, Luqiao Yin, Junchang Zhao, Ligang Xia, and Lifei Chen. “Exceptionally high thermal conductivity of thermal grease: Synergistic effects of graphene and alumina”. In: *International Journal of Thermal Sciences* 91 (2015), pp. 76–82. ISSN: 12900729. DOI: `10.1016/j.ijthermalsci.2015.01.006` (cit. on p. 13).

[62] Hongyuan Chen, Hanxing Wei, Minghai Chen, Fancheng Meng, Hongbo Li, and Qingwen Li. “Enhancing the effectiveness of silicone thermal grease by the addition of functionalized carbon nanotubes”. In: *Applied Surface Science* 283 (2013), pp. 525–531. ISSN: 01694332. DOI: `10.1016/j.apsusc.2013.06.139` (cit. on pp. 13, 16).

[63] Bui Hung Thang, Phan Ngoc Hong, Phan Hong Khoi, and Phan Ngoc Minh. “Application of multiwall carbon nanotubes for thermal dissipation in a microprocessor”. In: *Journal of Physics: Conference Series* 187 (2009), p. 012051. ISSN: 1742-6596. DOI: `10.1088/1742-6596/187/1/012051` (cit. on p. 13).

[64] Michael B. Jakubinek, Mary Anne White, Minfang Mu, and Karen I. Winey. “Temperature dependence of thermal conductivity enhancement in single-walled carbon nanotube/polystyrene composites”. In: *Applied Physics Letters* 96 (2010), pp. 94–97. ISSN: 00036951. DOI: `10.1063/1.3323095` (cit. on p. 14).

[65] Jinho Hong, Jeongwoo Lee, Chang Kook Hong, and Sang Eun Shim. “Effect of dispersion state of carbon nanotube on the thermal conductivity of poly(dimethyl siloxane) composites”. In: *Current Applied Physics* 10.1 (2010), pp. 359–363. ISSN: 15671739. DOI: `10.1016/j.cap.2009.06.028` (cit. on p. 14).

[66] Junpeng Li, Shuhua Qi, Mengyu Zhang, and Zhaofu Wang. “Thermal conductivity and electromagnetic shielding effectiveness of composites based on Ag-plating carbon fiber and epoxy”. In: *Journal of Applied Polymer Science* 132.33 (2015), n/a–n/a. ISSN: 00218995. DOI: `10.1002/app.42306` (cit. on p. 14).

[67] Kojiro Uetani, Seisuke Ata, Shigeki Tomonoh, Takeo Yamada, Motoo Yumura, and Kenji Hata. “Elastomeric Thermal Interface Materials with High Through-Plane Thermal Conductivity from Carbon Fiber Fillers Vertically Aligned by Electrostatic Flocking”. In: *Advanced Materials* 26.33 (2014), pp. 5857–5862. ISSN: 09359648. DOI: `10.1002/adma.201401736` (cit. on p. 14).

[68] Seung Hee Jeong, Si Chen, Jinxing Huo, Erik Kristofer Gamstedt, Johan Liu, Shi-Li Zhang, Zhi-Bin Zhang, Klas Hjort, and Zhigang Wu. “Mechanically Stretchable and Electrically Insulating Thermal Elastomer Composite by Liquid Alloy Droplet Embedment”. In: *Scientific Reports* 5.November (2015), p. 18257. ISSN: 2045-2322. DOI: `10.1038/srep18257` (cit. on p. 14).

[69] P Bonnet, D Sireude, B Garnier, and O Chauvet. “Thermal properties and percolation in carbon nanotube-polymer composites”. In: *Applied Physics Letters* 91.20 (2007), p. 201910. ISSN: 00036951. DOI: `10.1063/1.2813625` (cit. on p. 14).

[70] Chao Yuan, Bin Duan, Lan Li, Bin Xie, Mengyu Huang, and Xiaobing Luo. “Thermal Conductivity of Polymer-Based Composites with Magnetic Aligned Hexagonal Boron Nitride Platelets.” In: *ACS applied materials & interfaces* 7.23 (2015), pp. 13000–6. ISSN: 1944-8252. DOI: `10.1021/acsami.5b03007` (cit. on p. 14).

[71] Sang Woo Kim, Hyun-seok Choi, and Kyung-sub Lee. “Thermal conductivity of thermally conductive composites consisting of core–shell particles with nanostructured shell layers”. In: *Materials Research Bulletin* 60 (2014), pp. 843–848. ISSN: 00255408. DOI: `10.1016/j.materresbull.2014.09.079` (cit. on p. 14).

[72] THE EUROPEAN PARLIAMENT AND THE COUNCIL OF THE EUROPEAN UNION. “DIRECTIVE 2002/95/EC OF THE EUROPEAN PARLIAMENT AND OF THE COUNCIL”. In: *Official Journal of the European Union* 37 (2003), pp. 19–23 (cit. on p. 14).

[73] K Stinson-Bagby, D Huff, D Katsis, D Van Wyk, and G Q Lu. “Thermal performance and microstructure of lead versus lead-free solder die attach interface in power device packages”. In: *Electronics and the Environment, 2004. Conference Record. 2004 IEEE International Symposium on* (2004), pp. 27–32. ISSN: 1095-2020. DOI: `10.1109/ISEE.2004.1299683` (cit. on p. 15).

[74] Hiren R. Kotadia, Philip D. Howes, and Samjid H. Mannan. “A review: On the development of low melting temperature Pb-free solders”. In: *Microelectronics Reliability* 54.6-7 (2014), pp. 1253–1273. ISSN: 00262714. DOI: `10.1016/j.microrel.2014.02.025` (cit. on p. 15).

[75] Sean S. Too, Maxat Touzelbaev, Mohammad Khan, Raj Master, Jacquana Diep, and Kee-Hean Keok. “Indium thermal interface material development for microprocessors”. In: *2009 25th Annual IEEE Semiconductor Thermal Measurement and Management Symposium* (2009), pp. 186–192. DOI: `10.1109/STHERM.2009.4810762` (cit. on p. 15).

[76] Carl Deppisch, Thomas Fitzgerald, Arun Raman, Fay Hua, Charles Zhang, Pilin Liu, and Mikel Miller. “The material optimization and reliability characterization of an indium-solder thermal interface material for CPU packaging”. In: *Jom* 58.6 (2006), pp. 67–74. ISSN: 10474838. DOI: `10.1007/s11837-006-0186-6` (cit. on p. 15).

[77] T E Graedel, E M Harper, N T Nassar, Philip Nuss, and Barbara K Reck. "Criticality of metals and metalloids". In: *Proceedings of the National Academy of Sciences of the United States of America* 112.14 (2015), pp. 4257–4262. DOI: `10.1073/pnas.1500415112` (cit. on p. 15).

[78] Mathias Ekpu, Raj Bhatti, Michael I. Okereke, Sabuj Mallik, and Kenny Otiaba. "Fatigue life of lead-free solder thermal interface materials at varying bond line thickness in microelectronics". In: *Microelectronics Reliability* 54.1 (2014), pp. 239–244. ISSN: 00262714. DOI: `10.1016/j.microrel.2013.08.006` (cit. on p. 15).

[79] Rui Zhang, Jian Cai, Qian Wang, Jingwei Li, Yang Hu, Hongda Du, and Liangliang Li. "Thermal Resistance Analysis of Sn-Bi Solder Paste Used as Thermal Interface Material for Power Electronics Applications". In: *Journal of Electronic Packaging* 136.1 (2014), p. 011012. ISSN: 1043-7398. DOI: `10.1115/1.4026616` (cit. on pp. 15, 16, 36).

[80] Yunxia Gao and Jing Liu. "Gallium-based thermal interface material with high compliance and wettability". In: *Applied Physics A: Materials Science & Processing* 107.3 (2012), pp. 701–708. ISSN: 0947-8396. DOI: `10.1007/s00339-012-6887-5` (cit. on pp. 15, 16, 36).

[81] Chandan K. Roy, Sushil Bhavnani, Michael C. Hamilton, R. Wayne Johnson, Jonathan L. Nguyen, Roy W. Knight, and Daniel K. Harris. "Investigation into the application of low melting temperature alloys as wet thermal interface materials". In: *International Journal of Heat and Mass Transfer* 85 (2015), pp. 996–1002. ISSN: 00179310. DOI: `10.1016/j.ijheatmasstransfer.2015.02.029` (cit. on pp. 15, 16, 36).

[82] E. Yang, Hongyan Guo, Jingdong Guo, Jianku Shang, and Mingguang Wang. "Thermal Performance of Low-Melting-Temperature Alloy Thermal Interface Materials". In: *Acta Metallurgica Sinica (English Letters)* 27.2 (2014), pp. 290–294. ISSN: 1006-7191. DOI: `10.1007/s40195-014-0042-6` (cit. on p. 15).

[83] Yue-Guang Deng and Jing Liu. "Corrosion development between liquid gallium and four typical metal substrates used in chip cooling device". In: *Applied Physics A* 95.3 (2009), pp. 907–915. ISSN: 0947-8396. DOI: `10.1007/s00339-009-5098-1` (cit. on p. 15).

[84] Hui Yu, Liangliang Li, and Yujun Zhang. "Silver nanoparticle-based thermal interface materials with ultra-low thermal resistance for power electronics applications". In: *Scripta Materialia* 66.11 (2012), pp. 931–934. ISSN: 13596462. DOI: `10.1016/j.scriptamat.2012.02.037` (cit. on pp. 15, 16, 36).

[85] I Dutta, R Raj, P Kumar, T Chen, C M Nagaraj, J Liu, M Renavikar, and V Wakharkar. "Liquid phase sintered solders with indium as minority phase for next generation thermal interface material applications". In: *Journal of Electronic Materials* 38.12 (2009), pp. 2735–2745. ISSN: 0361-5235. DOI: `10.1007/s11664-009-0898-9` (cit. on pp. 15, 16).

[86] J Liu, P Kumar, I Dutta, R Raj, R Sidhu, M Renavikar, and R Mahajan. “Liquid phase sintered Cu – In composite solders for thermal interface material and interconnect applications”. In: *Journal of Materials Science* 46 (2011), pp. 7012–7025. ISSN: 0022-2461. DOI: `10.1007/s10853-011-5670-x` (cit. on p. 15).

[87] J. Liu, U. Sahaym, I. Dutta, R. Raj, M. Renavikar, R. S. Sidhu, and R. Mahajan. “Interfacially engineered liquid-phase-sintered Cu–In composite solders for thermal interface material applications”. In: *Journal of Materials Science* 49.22 (2014), pp. 7844–7854. ISSN: 0022-2461. DOI: `10.1007/s10853-014-8495-6` (cit. on pp. 16, 36, 37).

[88] P. Kumar and S. Awasthi. “Mechanical and thermal modeling of In-Cu composites for thermal interface materials applications”. In: *Journal of Composite Materials* 48.11 (2013), pp. 1391–1398. ISSN: 0021-9983. DOI: `10.1177/0021998313486502` (cit. on p. 16).

[89] Pulugurtha Markondeya Raj, Prashant Reddy Gangidi, Nikhilesh Nataraj, Nitesh Kumbhat, Gopal C Jha, Rao Tummala, and Nathaniel Brese. “Co-electrodeposited Solder Composite Films for Advanced Thermal Interface Materials”. In: *IEEE Transactions on Components, Packaging and Manufacturing Technology* 3.6 (2013), pp. 989–996 (cit. on p. 16).

[90] N Nagabandi, C Yegin, X Feng, C King, J K Oh, E A Scholar, S Narumanchi, and M Akbulut. “Chemically linked metal-matrix nanocomposites of boron nitride nanosheets and silver as thermal interface materials”. In: *Nanotechnology* 29.10 (2018). DOI: `https://doi.org/10.1088/1361-6528/aaa668` (cit. on p. 16).

[91] S. M L Nai, J. Wei, and M. Gupta. “Improving the performance of lead-free solder reinforced with multi-walled carbon nanotubes”. In: *Materials Science and Engineering A* 423.1-2 (2006), pp. 166–169. ISSN: 09215093. DOI: `10.1016/j.msea.2005.10.072` (cit. on p. 16).

[92] Li Yang, Chengchao Du, Jun Dai, Ning Zhang, and Yanfeng Jing. “Effect of nanosized graphite on properties of Sn-Bi solder”. In: *Journal of Materials Science: Materials in Electronics* 24.11 (2013), pp. 4180–4185. ISSN: 09574522. DOI: `10.1007/s10854-013-1380-2` (cit. on p. 16).

[93] Hiren R Kotadia, Arunkumar Panneerselvam, Mark W Sugden, Hector Steen, Mark Green, Samjid H Mannan, and Senior Member. “Electronics Assembly and High Temperature Paste With Zn Additives”. In: *IEEE Transactions on Components, Packaging and Manufacturing Technology* 3.10 (2013), pp. 1786–1793 (cit. on p. 16).

[94] Huizhen Huang, Xiuqin Wei, Fuping Liao, and Lang Zhou. “Preparation and properties of particle reinforced Sn-Zn-based composite solder”. In: *Journal Wuhan University of Technology, Materials Science Edition* 24.2 (2009), pp. 206–209. ISSN: 10002413. DOI: `10.1007/s11595-009-2206-1` (cit. on p. 16).

[95] Munish Sharma and D. D. L. Chung. “Solder–Graphite Network Composite Sheets as High-Performance Thermal Interface Materials”. In: *Journal of Electronic Materials* 44.3 (2015), pp. 929–947. ISSN: 0361-5235. DOI: `10.1007/s11664-014-3589-0` (cit. on pp. 16, 36).

[96] Hsiu-Hung Chen, Yuan Zhao, and Chung-Lung Chen. “Experimental Study of Coefficient of Thermal Expansion of Aligned Graphite Thermal Interface Materials”. In: *Frontiers in Heat and Mass Transfer* 4.1 (2013), pp. 1–7. ISSN: 2151-8629. DOI: `10.5098/hmt.v4.1.3004` (cit. on p. 16).

[97] Carl Zandén, Xin Luo, Lilei Ye, and Johan Liu. “A new solder matrix nano polymer composite for thermal management applications”. In: *Composites Science and Technology* 94 (2014), pp. 54–61. ISSN: 02663538. DOI: `10.1016/j.compscitech.2014.01.015` (cit. on pp. 16, 26, 31, 33).

[98] Murali Murugesan, Carl Zandén, Xin Luo, Lilei Ye, Valdas Jokubavicius, Mikael Syväjärvi, and Johan Liu. “A carbon fiber solder matrix composite for thermal management of microelectronic devices”. In: *Journal of Materials Chemistry C* 2.35 (2014), p. 7184. ISSN: 2050-7526. DOI: `10.1039/C4TC00936C` (cit. on pp. 16, 26, 28).

[99] Baratunde a. Cola, Timothy S. Fisher, and Xianfan Xu. “Carbon Nanotube Array Thermal Interfaces”. In: *Carbon Nanotubes: New Research.* New York: Nova Publishers, 2009. ISBN: 978-1-60692-236-1 (cit. on p. 17).

[100] Mukul Kumar and Yoshinori Ando. “Chemical Vapor Deposition of Carbon Nanotubes: A Review on Growth Mechanism and Mass Production”. In: *Journal of Nanoscience and Nanotechnology* 10.6 (2010), pp. 3739–3758. ISSN: 15334880. DOI: `10.1166/jnn.2010.2939` (cit. on pp. 17, 19, 20).

[101] Amy M. Marconnet, Matthew a. Panzer, and Kenneth E. Goodson. “Thermal conduction phenomena in carbon nanotubes and related nanostructured materials”. In: *Reviews of Modern Physics* 85.3 (2013), pp. 1295–1326. ISSN: 00346861. DOI: `10.1103/RevModPhys.85.1295` (cit. on p. 17).

[102] Baratunde a. Cola, Jun Xu, and Timothy S. Fisher. “Contact mechanics and thermal conductance of carbon nanotube array interfaces”. In: *International Journal of Heat and Mass Transfer* 52.15-16 (2009), pp. 3490–3503. ISSN: 00179310. DOI: `10.1016/j.ijheatmasstransfer.2009.03.011` (cit. on p. 17).

[103] Tao Tong, Yang Zhao, L. Delzeit, A. Kashani, M. Meyyappan, and A. Majumdar. “Dense Vertically Aligned Multiwalled Carbon Nanotube Arrays as Thermal Interface Materials”. In: *IEEE Transactions on Components and Packaging Technologies* 30.1 (2007), pp. 92–100. ISSN: 1521-3331. DOI: `10.1109/TCAPT.2007.892079` (cit. on pp. 17, 18).

[104] M. a. Panzer, G. Zhang, D. Mann, X. Hu, E. Pop, H. Dai, and K. E. Goodson. “Thermal Properties of Metal-Coated Vertically Aligned Single-Wall Nanotube Arrays”. In: *Journal of Heat Transfer* 130.5 (2008), p. 052401. ISSN: 00221481. DOI: `10.1115/1.2885159` (cit. on pp. 17, 18).

[105] Baratunde a. Cola, Jun Xu, Changrui Cheng, Xianfan Xu, Timothy S. Fisher, and Hanping Hu. “Photoacoustic characterization of carbon nanotube array thermal interfaces”. In: *Journal of Applied Physics* 101.5 (2007), pp. 1–9. ISSN: 00218979. DOI: `10.1063/1.2510998` (cit. on p. 17).

[106] Matthew A. Panzer, Hai M. Duong, Jun Okawa, Junichiro Shiomi, Brian L. Wardle, Shigeo Maruyama, and Kenneth E. Goodson. “Temperature-dependent phonon conduction and nanotube engagement in metalized single wall carbon nanotube films”. In: *Nano Letters* 10.7 (2010), pp. 2395–2400. ISSN: 15306984. DOI: `10.1021/nl100443x` (cit. on p. 18).

[107] Qingwei Li, Changnong Liu, and Shoushan Fan. “Thermal boundary resistances of carbon nanotubes in contact with metals and polymers”. In: *Nano Letters* 9 (2009), pp. 3805–3809. ISSN: 15306984. DOI: `10.1021/nl901988t` (cit. on p. 18).

[108] Yagang Yao, Ju Nie Tey, Zhuo Li, Jun Wei, Kathleen Bennett, Andrew McNamara, Yogendra Joshi, Rachel Lee Siew Tan, Sharon Nai Mui Ling, and Ching Ping Wong. “High-quality vertically aligned carbon nanotubes for applications as thermal interface materials”. In: *IEEE Transactions on Components, Packaging and Manufacturing Technology* 4.2 (2014), pp. 232–239. ISSN: 21563950. DOI: `10.1109/TCPMT.2013.2296370` (cit. on p. 18).

[109] Baratunde a. Cola, Placidus B. Amama, Xianfan Xu, and Timothy S. Fisher. “Effects of Growth Temperature on Carbon Nanotube Array Thermal Interfaces”. In: *Journal of Heat Transfer* 130 (2008), p. 114503. ISSN: 00221481. DOI: `10.1115/1.2969758` (cit. on pp. 18, 19, 37).

[110] P B Amama, B A Cola, T D Sands, X F Xu, and T S Fisher. “Dendrimer-assisted controlled growth of carbon nanotubes for enhanced thermal interface conductance”. In: *Nanotechnology* 18.38 (2007), p. 385303. ISSN: 0957-4484. DOI: `10.1088/0957-4484/18/38/385303` (cit. on p. 18).

[111] Xi Liu, Yi Zhang, Alan M. Cassell, and Brett a. Cruden. “Implications of catalyst control for carbon nanotube based thermal interface materials”. In: *Journal of Applied Physics* 104.8 (2008), p. 084310. ISSN: 00218979. DOI: `10.1063/1.2999644` (cit. on p. 18).

[112] Robert Cross, Baratunde a Cola, Timothy Fisher, Xianfan Xu, Ken Gall, and Samuel Graham. “A metallization and bonding approach for high performance carbon nanotube thermal interface materials.” In: *Nanotechnology* 21.44 (2010), p. 445705. ISSN: 0957-4484. DOI: `10.1088/0957-4484/21/44/445705` (cit. on pp. 18, 20).

[113] Stephen L Hodson, Thiruvelu Bhuvana, Baratunde A Cola, Xianfan Xu, G U Kulkarni, and Timothy S Fisher. “Palladium Thiolate Bonding of Carbon Nanotube Thermal Interfaces”. In: *Journal of Electronic Packaging* 133.2 (2011), p. 20907. ISSN: 1043-7398. DOI: `10.1115/1.4004094` (cit. on p. 18).

[114] Michael T Barako, Yuan Gao, Yoonjin Won, Amy M Marconnet, Mehdi Asheghi, and Kenneth E Goodson. “Reactive Metal Bonding of Carbon Nanotube Arrays for Thermal Interface Applications”. In: *IEEE Transactions on Components, Packaging and Manufacturing Technology* 4.12 (2014), pp. 1906–1913. ISSN: 2156-3950. DOI: `10.1109/TCPMT.2014.2369371` (cit. on p. 18).

[115] Yuxiang Ni, Hung Le Khanh, Yann Chalopin, Jinbo Bai, Pierre Lebarny, Laurent Divay, and Sebastian Volz. “Highly efficient thermal glue for carbon nanotubes based on azide polymers”. In: *Applied Physics Letters* 100.19 (2012), p. 193118. ISSN: 00036951. DOI: `10.1063/1.4711809` (cit. on p. 19).

[116] John H Taphouse, Thomas L Bougher, Virendra Singh, Parisa Pour Shahid Saeed Abadi, Samuel Graham, and Baratunde A Cola. “Carbon nanotube thermal interfaces enhanced with sprayed on nanoscale polymer coatings”. In: *Nanotechnology* 24.10 (2013), p. 105401. ISSN: 0957-4484. DOI: `10.1088/0957-4484/24/10/105401` (cit. on p. 19).

[117] J Daon et al. “Electrically conductive thermal interface materials based on vertically aligned carbon nanotubes mats”. In: *Therminic 20th International workshop*. 2014, pp. 1–4. ISBN: 9781479954155. DOI: `10.1109/THERMINIC.2014.6972534` (cit. on p. 19).

[118] Wei Lin, Rongwei Zhang, Kyoung-Sik Moon, and C.P. Wong. “Molecular phonon couplers at carbon nanotube/substrate interface to enhance interfacial thermal transport”. In: *Carbon* 48.1 (2010), pp. 107–113. ISSN: 00086223. DOI: `10.1016/j.carbon.2009.08.033` (cit. on p. 19).

[119] Sumanjeet Kaur, Nachiket Raravikar, Brett A. Helms, Ravi Prasher, and D. Frank Ogletree. “Enhanced thermal transport at covalently functionalized carbon nanotube array interfaces”. In: *Nature Communications* 5 (2014), pp. 1–8. ISSN: 2041-1723. DOI: `10.1038/ncomms4082` (cit. on p. 19).

[120] John H. Taphouse, O’Neil L. Smith, Seth R. Marder, and Baratunde a. Cola. “A pyrenylpropyl phosphonic acid surface modifier for mitigating the thermal resistance of carbon nanotube contacts”. In: *Advanced Functional Materials* 24.4 (2014), pp. 465–471. ISSN: 1616301X. DOI: `10.1002/adfm.201301714` (cit. on p. 19).

[121] Wei Lin, Rongwei Zhang, Kyoung Sik Moon, and C. P. Wong. “Synthesis of high-quality vertically aligned carbon nanotubes on bulk copper substrate for thermal management”. In: *IEEE Transactions on Advanced Packaging* 33.2 (2010), pp. 370–376. ISSN: 15213323. DOI: `10.1109/TADVP.2009.2034335` (cit. on p. 20).

[122] Z L Gao, K Zhang, and M M F Yuen. “Fabrication of carbon nanotube thermal interface material on aluminum alloy substrates with low pressure CVD.” In: *Nanotechnology* 22.26 (2011), p. 265611. ISSN: 0957-4484. DOI: `10.1088/0957-4484/22/26/265611` (cit. on p. 20).

[123] Zhang Kai, Matthew M F Yuen, David G W Xiao, Y. Y. Fu, and Philip Chan. “Directly synthesizing CNT-TIM on aluminum alloy heat sink for HB-LED thermal management”. In: *Proceedings - Electronic Components and Technology Conference* (2008), pp. 1659–1663. ISSN: 05695503. DOI: `10.1109/ECTC.2008.4550200` (cit. on p. 20).

[124] Ashavani Kumar, Victor L. Pushparaj, Swastik Kar, Omkaram Nalamasu, Pulickel M. Ajayan, and Rajashree Baskaran. “Contact transfer of aligned carbon nanotube arrays onto conducting substrates”. In: *Applied Physics Letters* 89.16 (2006), pp. 14–17. ISSN: 00036951. DOI: `10.1063/1.2356899` (cit. on p. 20).

[125] Yifeng Fu, Yiheng Qin, Teng Wang, Si Chen, and Johan Liu. “Ultrafast transfer of metal-enhanced carbon nanotubes at low temperature for large-scale electronics assembly”. In: *Advanced Materials* 22.44 (2010), pp. 5039–5042. ISSN: 09359648. DOI: `10.1002/adma.201002415` (cit. on p. 20).

[126] A Hamdan, J Cho, R Johnson, J Jiao, D Bahr, R Richards, and C Richards. “Evaluation of a thermal interface material fabricated using thermocompression bonding of carbon nanotube turf.” In: *Nanotechnology* 21.1 (2010), p. 015702. ISSN: 1361-6528. DOI: `10.1088/0957-4484/21/1/015702` (cit. on p. 20).

[127] M X Chen, X H Song, Z Y Gan, and S Liu. “Low temperature thermocompression bonding between aligned carbon nanotubes and metallized substrate.” In: *Nanotechnology* 22.34 (2011), p. 345704. ISSN: 1361-6528. DOI: `10.1088/0957-4484/22/34/345704` (cit. on p. 20).

[128] Baratunde a. Cola, Xianfan Xu, and Timothy S. Fisher. “Increased real contact in thermal interfaces: A carbon nanotube/foil material”. In: *Applied Physics Letters* 90.9 (2007), pp. 9–11. ISSN: 00036951. DOI: `10.1063/1.2644018` (cit. on p. 20).

[129] H. Wang, J. Y. Feng, X. J. Hu, and K. M. Ng. “Reducing thermal contact resistance using a bilayer aligned CNT thermal interface material”. In: *Chemical Engineering Science* 65.3 (2010), pp. 1101–1108. ISSN: 00092509. DOI: `10.1016/j.ces.2009.09.064` (cit. on p. 20).

[130] Nuri Na, Kei Hasegawa, Xiaosong Zhou, Mizuhisa Nihei, and Suguru Noda. “Denser and taller carbon nanotube arrays on Cu foils useable as thermal interface materials”. In: *Japanese Journal of Applied Physics* 54.9 (2015). ISSN: 13474065. DOI: `10.7567/JJAP.54.095102` (cit. on p. 20).

[131] Hua Huang, Changhong Liu, Yang Wu, and Shoushan Fan. “Aligned carbon nanotube composite films for thermal management”. In: *Advanced Materials* 17 (2005), pp. 1652–1656. ISSN: 09359648. DOI: `10.1002/adma.200500467` (cit. on p. 20).

[132] Amy M. Marconnet, Namiko Yamamoto, Matthew A. Panzer, Brian L. Wardle, and Kenneth E. Goodson. “Thermal conduction in aligned carbon nanotube-polymer nanocomposites with high packing density”. In: *ACS Nano* 5.6 (2011), pp. 4818–4825. ISSN: 19360851. DOI: `10.1021/nn200847u` (cit. on p. 20).

[133] Miao Wang et al. “Crack-free and scalable transfer of carbon nanotube arrays into flexible and highly thermal conductive composite film.” In: *ACS applied materials & interfaces* 6.1 (2014), pp. 539–44. ISSN: 1944-8252. DOI: `10.1021/am404594m` (cit. on p. 20).

[134] Y. T. Lee, S. Shanmugan, and D. Mutharasu. “Thermal resistance of CNTs-based thermal interface material for high power solid state device packages”. In: *Applied Physics A: Materials Science and Processing* 114.4 (2014), pp. 1145–1152. ISSN: 09478396. DOI: `10.1007/s00339-013-7676-5` (cit. on p. 20).

[135] Jun Xu and Timothy S. Fisher. “Enhancement of thermal interface materials with carbon nanotube arrays”. In: *International Journal of Heat and Mass Transfer* 49.9-10 (2006), pp. 1658–1666. ISSN: 00179310. DOI: `10.1016/j.ijheatmasstransfer.2005.09.039` (cit. on p. 20).

[136] K Zhang, Y Chai, M M F Yuen, D G W Xiao, and P C H Chan. “Carbon nanotube thermal interface material for high-brightness light-emitting-diode cooling.” In: *Nanotechnology* 19.21 (2008), p. 215706. ISSN: 0957-4484. DOI: `10.1088/0957-4484/19/21/215706` (cit. on p. 20).

[137] Baratunde a. Cola, Xianfan Xu, Timothy S. Fisher, Michael a. Capano, and Placidus B. Amama. “Carbon Nanotube Array Thermal Interfaces for High-Temperature Silicon Carbide Devices”. In: *Nanoscale and Microscale Thermophysical Engineering* 12.November (2008), pp. 228–237. ISSN: 1556-7265. DOI: `10.1080/15567260802183015` (cit. on p. 20).

[138] Michael T. Barako. “Solder-Bonded Carbon Nanotube Thermal Interface Materials”. In: *2012 13Th Ieee Intersociety Conference on Thermal and Thermomechanical Phenomena in Electronic Systems (Itherm)* (2012), pp. 1225–1233. ISSN: 19363958. DOI: `10.1109/ITHERM.2012.6231562` (cit. on p. 20).

[139] Joseph R Wasniewski, David H Altman, Stephen L Hodson, Timothy S Fisher, Anuradha Bulusu, Samuel Graham, and Baratunde A Cola. “Characterization of Metallically Bonded Carbon Nanotube-Based Thermal Interface Materials Using a High Accuracy 1D Steady-State Technique”. In: *Journal of Electronic Packaging* 134.2 (2012), p. 20901. ISSN: 1043-7398. DOI: `10.1115/1.4005909` (cit. on pp. 20, 22).

[140] Erik S Polsen, Daniel Q McNerny, B Viswanath, Sebastian W Pattinson, and A John Hart. “High-speed roll-to-roll manufacturing of graphene using a concentric tube CVD reactor.” In: *Scientific reports* 5 (2015), p. 10257. ISSN: 2045-2322. DOI: `10.1038/srep10257` (cit. on p. 21).

[141] Margarita R Arcila-velez, Jingyi Zhu, and Anthony Childress. “Roll-to-roll synthesis of vertically aligned carbon nanotube electrodes for electrical double layer capacitors”. In: *Nano Energy* 8 (2014), pp. 9–16. ISSN: 2211-2855. DOI: `10.1016/j.nanoen.2014.05.004` (cit. on p. 21).

[142] Roger Kempers, Anthony Robinson, and Lyons Alan. “Characterization of Metal Micro-Textured Thermal Interface Materials”. In: *Thermal Investigations of ICs and Systems, 2009. THERMINIC 2009. 15th International Workshop* November (2009) (cit. on p. 21).

[143] R. Kempers, a. M. Lyons, and a. J. Robinson. “Modeling and Experimental Characterization of Metal Microtextured Thermal Interface Materials”. In: *Journal of Heat Transfer* 136.1 (2013), p. 011301. ISSN: 0022-1481. DOI: `10.1115/1.4024737` (cit. on p. 21).

[144] R Kempers and S Kerslake. “In Situ Testing of Metal Micro-Textured Thermal Interface Materials in Telecommunications Applications”. In: *Journal of Physics: Conference Series* 525 (2014), p. 012016. ISSN: 1742-6588. DOI: `10.1088/1742-6596/525/1/012016` (cit. on p. 21).

[145] Bo Feng, Fardin Faruque, Peng Bao, An-Ting Chien, Satish Kumar, and G. P. Peterson. “Double-sided tin nanowire arrays for advanced thermal interface materials”. In: *Applied Physics Letters* 102.9 (2013), p. 093105. ISSN: 00036951. DOI: `10.1063/1.4791575` (cit. on p. 21).

[146] Michael T. Barako, Shilpi Roy-Panzer, Timothy S. English, Takashi Kodama, Mehdi Asheghi, Thomas W. Kenny, and Kenneth E. Goodson. “Thermal Conduction in Vertically Aligned Copper Nanowire Arrays and Composites”. In: *ACS Applied Materials & Interfaces* 7.34 (2015), pp. 19251–19259. ISSN: 1944-8244. DOI: `10.1021/acsami.5b05147` (cit. on p. 21).

[147] David Shaddock, Stanton Weaver, Ioannis Chasiotis, Binoy Shah, and Dalong Zhong. “Development of a Compliant Nanothermal Interface Material”. In: *ASME 2011 Pacific Rim Technical Conference and Exhibition on Packaging and Integration of Electronic and Photonic Systems, MEMS and NEMS: Volume 2*. ASME, 2011, pp. 13–17. ISBN: 978-0-7918-4462-5. DOI: `10.1115/IPACK2011-52015` (cit. on p. 21).

[148] Sheng Shen, Asegun Henry, Jonathan Tong, Ruiting Zheng, and Gang Chen. “Polyethylene nanofibres with very high thermal conductivities”. In: *Nature Nanotechnology* 5.4 (2010), pp. 251–255. ISSN: 1748-3387. DOI: `10.1038/nnano.2010.27` (cit. on p. 22).

[149] Virendra Singh et al. “High thermal conductivity of chain-oriented amorphous polythiophene”. In: *Nature Nanotechnology* 9.5 (2014), pp. 384–390. ISSN: 1748-3387. DOI: `10.1038/nnano.2014.44` (cit. on p. 22).

[150] Xinfeng Zhang et al. “Exceptional thermal interface properties of a three-dimensional graphene foam”. In: *Carbon* 66 (2014), pp. 201–209. ISSN: 00086223. DOI: `10.1016/j.carbon.2013.08.059` (cit. on p. 22).

[151] Peng Lv, Xiao-Wen Tan, Ke-Han Yu, Rui-Lin Zheng, Jia-Jin Zheng, and Wei Wei. “Super-elastic graphene/carbon nanotube aerogel: A novel thermal interface material with highly thermal transport properties”. In: *Carbon* 99 (2016), pp. 222–228. ISSN: 00086223. DOI: `10.1016/j.carbon.2015.12.026` (cit. on p. 22).

[152] Yong Zhang, Haoxue Han, Nan Wang, Pengtu Zhang, Yifeng Fu, Murali Murugesan, Michael Edwards, Kjell Jeppson, Sebastian Volz, and Johan Liu. “Improved Heat Spreading Performance of Functionalized Graphene in Microelectronic Device Application”. In: *Advanced Functional Materials* 25.28 (2015), pp. 4430–4435. ISSN: 16163028. DOI: `10.1002/adfm.201500990` (cit. on p. 22).

[153] Qizhen Liang, Xuxia Yao, Wei Wang, Yan Liu, and Ching Ping Wong. “A three-dimensional vertically aligned functionalized multilayer graphene architecture: An approach for graphene-based thermal interfacial materials”. In: *ACS Nano* 5.3 (2011), pp. 2392–2401. ISSN: 19360851. DOI: `10.1021/nn200181e` (cit. on p. 22).

[154] Xingyi Huang, Chunyi Zhi, Pingkai Jiang, Dmitri Golberg, Yoshio Bando, and Toshikatsu Tanaka. “Polyhedral oligosilsesquioxane-modified boron nitride nanotube based epoxy nanocomposites: An ideal dielectric material with high thermal conductivity”. In: *Advanced Functional Materials* 23.14 (2013), pp. 1824–1831. ISSN: 1616301X. DOI: `10.1002/adfm.201201824` (cit. on p. 22).

[155] Manuela Loeblein, Siu Hon Tsang, Yong Han, Xiaowu Zhang, Edwin Hang, and Tong Teo. “Heat Dissipation Enhancement of 2 . 5D Package with 3D Graphene & 3D Boron Nitride Networks as Thermal Interface Material (TIM)”. In: *2016 IEEE 66th Electronic Components and Technology Conference*. 2016, pp. 707–713. ISBN: 9781509012046. DOI: `10.1109/ECTC.2016.85` (cit. on p. 22).

[156] Gou Yujun, Liu Zhongliang, Zhang Guangmeng, and Li Yanxia. “Effects of multi-walled carbon nanotubes addition on thermal properties of thermal grease”. In: *International Journal of Heat and Mass Transfer* 74 (2014), pp. 358–367. ISSN: 00179310. DOI: `10.1016/j.ijheatmasstransfer.2014.03.009` (cit. on p. 22).

[157] Hongyuan Chen, Minghai Chen, Jiangtao Di, Geng Xu, Hongbo Li, and Qingwen Li. “Architecting three-dimensional networks in carbon nanotube buckypapers for thermal interface materials”. In: *Journal of Physical Chemistry C* 116.6 (2012), pp. 3903–3909. ISSN: 19327447. DOI: `10.1021/jp2086158` (cit. on p. 22).

[158] Ronald J. Warzoha, Di Zhang, Gang Feng, and Amy S. Fleischer. “Engineering interfaces in carbon nanostructured mats for the creation of energy efficient thermal interface materials”. In: *Carbon* 61 (2013), pp. 441–457. ISSN: 00086223. DOI: `10.1016/j.carbon.2013.05.028` (cit. on p. 22).

[159] Kesong Hu and D. D L Chung. “Flexible graphite modified by carbon black paste for use as a thermal interface material”. In: *Carbon* 49.4 (2011), pp. 1075–1086. ISSN: 00086223. DOI: `10.1016/j.carbon.2010.10.058` (cit. on p. 22).

[160] Yasuhiro Aoyagi and D. D L Chung. "Antioxidant-based phase-change thermal interface materials with high thermal stability". In: *Journal of Electronic Materials* 37.4 (2008), pp. 448–461. ISSN: 03615235. DOI: `10.1007/s11664-007-0376-1` (cit. on p. 22).

[161] Björn Carlberg, Teng Wang, Yifeng Fu, Johan Liu, and Dongkai Shangguan. "Nanostructured Polymer-Metal Composite for Thermal Interface Material Applications". In: *58th Electronic Components and Technology Conference (ECTC), 2008.* 2008, pp. 191–197. ISBN: 9781424422319. DOI: `10.1109/ECTC.2008.4549969` (cit. on pp. 25, 26).

[162] Xin Luo, Yong Zhang, Carl Zandén, Murali Murugesan, Yu Cao, Lilei Ye, and Johan Liu. "Novel thermal interface materials: Boron nitride nanofiber and indium composites for electronics heat dissipation applications". In: *Journal of Materials Science: Materials in Electronics* 25.5 (2014), pp. 2333–2338. ISSN: 1573482X. DOI: `10.1007/s10854-014-1880-8` (cit. on pp. 26, 33).

[163] Björn Carlberg, Teng Wang, Johan Liu, and Dongkai Shangguan. "Polymer-metal nano-composite films for thermal management". In: *Microelectronics International* 26.2 (2009), pp. 28–36. ISSN: 1356-5362. DOI: `10.1108/13565360910960213` (cit. on pp. 26, 29).

[164] Carl Zandén, Xin Luo, Lilei Ye, and Johan Liu. "Fabrication and characterization of a metal matrix polymer fibre composite for thermal interface material applications". In: *19th International Workshop on Thermal Investigations of ICs and Systems (THERMINIC)* 2013 (2013), pp. 286–292. DOI: `10.1109/THERMINIC.2013.6675196` (cit. on pp. 26, 29).

[165] Shuangxi Sun, Si Chen, Xin Luo, Yifeng Fu, Lilei Ye, and Johan Liu. "Mechanical and thermal characterization of a novel nanocomposite thermal interface material for electronic packaging". In: *Microelectronics Reliability* 56 (2015), pp. 129–135. ISSN: 00262714. DOI: `10.1016/j.microrel.2015.10.028` (cit. on pp. 26, 29, 31).

[166] G Kaptay. "The threshold pressure of infiltration into fibrous preforms normal to the fibers ' axes". In: *Composites Science and Technology* 68 (2008), pp. 228–237. DOI: `10.1016/j.compscitech.2007.04.023` (cit. on p. 26).

[167] C. Pradere, J. C. Batsale, J. M. Goyhénèche, R. Pailler, and S. Dilhaire. "Thermal properties of carbon fibers at very high temperature". In: *Carbon* 47.3 (2009), pp. 737–743. ISSN: 00086223. DOI: `10.1016/j.carbon.2008.11.015` (cit. on p. 28).

[168] Yu. V. Naidich and G. A. Kolesnichenko. "Investigation of the wetting of diamond and graphite by molten metals and alloys V. Carbide-formation kinetics at the graphite/metallic melt interface". In: *Soviet Powder Metallurgy and Metal Ceramics* 7.2 (Feb. 1968), pp. 139–141. ISSN: 0038-5735. DOI: `10.1007/BF00774308` (cit. on p. 28).

[169] Alexander Hanss, E Liu, Maximilian Schmid, and Gordon Elger. "The influence of voids in solder joints on thermal performance and reliability investigated with transient thermal analysis". In: *21st International Workshop on Thermal Investigations of ICs and Systems (THERMINIC)*. Paris, France: IEEE, 2015, pp. 1–6. ISBN: 9781467397056. DOI: `10.1109/THERMINIC.2015.7389623` (cit. on p. 31).

[170] Karl Seelig and Kevin Pigeon. "Overcoming the challenges of the QFN package". In: *SMTA International Conference Proceedings*. 2011 (cit. on p. 31).

[171] Kenny C Otiaba, M I Okereke, and R S Bhatti. "Numerical assessment of the effect of void morphology on thermo- mechanical performance of solder thermal interface material". In: *Applied Thermal Engineering* 64.1-2 (2014), pp. 51–63. ISSN: 1359-4311. DOI: `10.1016/j.applthermaleng.2013.12.006` (cit. on p. 31).

[172] Indium Corporation. *Thermal K Values List*. URL: `http://www.indium.com/thermal-management/thermal-k-list/` (visited on 11/30/2017) (cit. on p. 32).

[173] Hyoung Seop Kim and Mark B Bush. "The effects of grain size and porosity on the elastic modulus of nanocrystalline materials". In: 11.3 (1999), pp. 361–367 (cit. on p. 33).

[174] A Shubert, H Walter, R Dudek, B Michel, G Lefranc, J Otto, and G Mitic. "Thermo- mechanical properties and creep deformation of lead-containing and lead-free solders". In: *2001 International Symposium on Advanced Packaging Materials*. 2001, pp. 129–134 (cit. on p. 33).

[175] M Klein, A Hadrboletz, B Weiss, and G Khatibi. "The 'size effect' on the stress – strain, fatigue and fracture properties of thin metallic foils". In: *Materials Science and Engineering A* 321 (2001), pp. 924–928 (cit. on p. 33).

[176] Y T Zhu. "Microstructures and mechanical properties of ultrafine-grained Ti foil processed by equal-channel angular pressing and cold rolling". In: (2017) (cit. on p. 33).

[177] Meng Song, Xianghua Liu, and Lizhong Liu. "Size Effect on Mechanical Properties and Texture of Pure Copper Foil by Cold Rolling". In: (2017), pp. 1–18. DOI: `10.3390/ma10050538` (cit. on p. 33).

[178] A Diehl, U Engel, and M Geiger. "Mechanical properties and bending behaviour of metal foils". In: 222 (2007), pp. 83–91. DOI: `10.1243/09544054JEM838` (cit. on p. 33).

[179] Avram Bar-Cohen, Kaiser Matin, and Sreekant Narumanchi. "Nanothermal Interface Materials: Technology Review and Recent Results". In: *Journal of Electronic Packaging* 137.4 (2015), p. 040803. ISSN: 1043-7398. DOI: `10.1115/1.4031602` (cit. on p. 37).